



Search for R -parity violating supersymmetry with displaced vertices in proton-proton collisions at $\sqrt{s} = 8$ TeV

The CMS Collaboration*

Abstract

Results are reported from a search for R -parity violating supersymmetry in proton-proton collision events collected by the CMS experiment at a center-of-mass energy of $\sqrt{s} = 8$ TeV. The data sample corresponds to an integrated luminosity of 17.6 fb^{-1} . This search assumes a minimal flavor violating model in which the lightest supersymmetric particle is a long-lived neutralino or gluino, leading to a signal with jets emanating from displaced vertices. In a sample of events with two displaced vertices, no excess yield above the expectation from standard model processes is observed, and limits are placed on the pair production cross section as a function of mass and lifetime of the neutralino or gluino. At 95% confidence level, the analysis excludes cross sections above approximately 1 fb for neutralinos or gluinos with mass between 400 and 1500 GeV and mean proper decay length between 1 and 30 mm. Gluino masses are excluded below 1 and 1.3 TeV for mean proper decay lengths of $300 \mu\text{m}$ and 1 mm, respectively, and below 1.4 TeV for the range 2–30 mm. The results are also applicable to other models in which long-lived particles decay into multijet final states.

Published in Physical Review D as doi:10.1103/PhysRevD.95.01.012009.

1 Introduction

In spite of extensive efforts by the ATLAS and CMS Collaborations at the CERN LHC, the superpartners of standard model (SM) particles predicted by supersymmetry (SUSY) [1, 2] have not yet been observed. If superpartners are produced and R -parity [3] is conserved, the lightest supersymmetric particle (LSP) passes through the detector unobserved, except for a potentially large amount of missing transverse energy. The assumption of R -parity conservation is motivated by experimental observations such as limits on the proton lifetime [4]. This assumption is not strictly required as long as either lepton or baryon number is conserved, or the associated R -parity violating (RPV) [5] terms in the Lagrangian are extremely small. Searches for a variety of signatures have not yet found any evidence for RPV SUSY [6–10].

In minimal flavor violating (MFV) models of RPV SUSY [11, 12], the Yukawa couplings between superpartners and SM particles are the sole source of flavor symmetry violation, and the amplitudes for lepton- and baryon-number changing interactions are correspondingly small. At the LHC, the LSP typically decays within the detector volume, so there is no large missing transverse energy. The production processes of the superpartners are similar to those in the minimal supersymmetric standard model in that superpartners are produced in pairs, but the phenomenology depends on the identity of the LSP.

This analysis uses a benchmark signal model described in Ref. [12], in which the LSP is assumed to be either a neutralino or a gluino that is sufficiently heavy to decay into a top antiquark and a virtual top squark. The virtual top squark then decays via a baryon-number violating process to strange and bottom antiquarks, as shown in Fig. 1. Although this decay is heavily suppressed by the Yukawa coupling, it still dominates the top squark rate, with other partial widths being suppressed by a factor of 100 or more. As a consequence, the LSP is long-lived, with a lifetime that depends on the model parameters. For large parts of the parameter space, pair-produced LSPs lead to interesting signatures. Observable effects include increased top quark production rates; events with many jets, especially b quark jets; and events with displaced vertices.

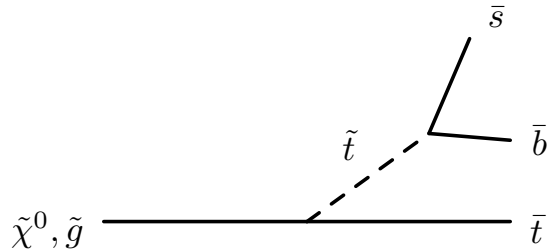


Figure 1: Decay diagram for the pair-produced neutralino ($\tilde{\chi}^0$) or gluino (\tilde{g}) LSP in the assumed signal model. In both cases, the LSP decays into a top antiquark plus a virtual top squark (\tilde{t}); the top squark then decays via a baryon-number violating process into strange and bottom antiquarks.

The decay of the LSP results in multiple jets emerging from a displaced vertex, often with wide opening angles. To identify the displaced vertices, we use a custom vertex reconstruction algorithm optimized for these distinctive features. This algorithm differs from standard methods used to identify b quark jets [13], which assume a single jet whose momentum is aligned with the vertex displacement from the primary vertex. Our signature consists of two vertices, well separated in space. Studies based on event samples from Monte Carlo (MC) simulation show that SM background events rarely contain even one such reconstructed displaced vertex. In the even rarer events with two displaced vertices, the vertices are usually not well separated from

each other.

The CMS Collaboration has also searched for pairs of displaced jets from a single vertex [14], while this analysis searches for a pair of displaced vertices, each of which is associated with a jet. The study reported here is sensitive to mean proper decay lengths between $300\ \mu\text{m}$ and $30\ \text{mm}$, which are shorter than those probed by a similar analysis performed by the ATLAS Collaboration [15], and longer than those probed by a CMS analysis that looked for prompt LSP decays based on the jet and b-tagged jet multiplicity distributions [10].

This analysis applies not only to the MFV model described here, but more generally to models for physics beyond the SM with long-lived particles decaying to multiple jets. In addition to the results of the search with a neutralino or gluino LSP, we present a method for reinterpretation of the analysis.

2 The CMS detector

The central feature of the CMS detector is a superconducting solenoid providing a magnetic field of $3.8\ \text{T}$ aligned with the proton beam direction. Contained within the field volume of the solenoid are a silicon pixel and strip tracker, a lead tungstate electromagnetic calorimeter (ECAL), and a brass and scintillator hadronic calorimeter (HCAL). Outside the solenoid is the steel magnetic return yoke interspersed with muon tracking chambers. A more detailed description of the CMS detector, together with a definition of the coordinate system used and the relevant kinematic variables, can be found in Ref. [16].

The silicon tracker, which is particularly relevant to this analysis, measures the tracks of charged particles in the range of pseudorapidity, η , up to $|\eta| < 2.5$. For nonisolated particles with transverse momentum, p_T , of 1 to $10\ \text{GeV}$ and $|\eta| < 1.4$, the track resolutions are typically 1.5% in p_T , 25 – $90\ \mu\text{m}$ in the impact parameter in the transverse plane, and 45 – $150\ \mu\text{m}$ in the impact parameter in the longitudinal direction [17]. When combining information from the entire detector, the jet energy resolution amounts typically to 15% at $10\ \text{GeV}$, 8% at $100\ \text{GeV}$, and 4% at $1\ \text{TeV}$, to be compared to about 40% , 12% , and 5% obtained when the ECAL and HCAL calorimeters alone are used [18].

The first level (L1) of the CMS trigger system, which is composed of custom hardware processors, uses information from the calorimeters and muon detectors to select the most interesting events in a fixed time interval of less than $4\ \mu\text{s}$. The high-level trigger (HLT) processor farm further decreases the event rate from around $100\ \text{kHz}$ to less than $1\ \text{kHz}$, before data storage.

3 Event samples

The data sample used in this analysis corresponds to an integrated luminosity of $17.6\ \text{fb}^{-1}$, collected in proton-proton (pp) collisions at a center-of-mass energy of $\sqrt{s} = 8\ \text{TeV}$ in 2012. Events are selected using a trigger requiring the presence of at least four jets reconstructed from energy deposits in the calorimeters. At the L1 trigger, the jets are required to have $p_T > 40\ \text{GeV}$, while in the HLT the threshold is $p_T > 50\ \text{GeV}$. The latter threshold is afforded by a special data-taking strategy called “data parking” [19], in which the triggered events were saved but not promptly reconstructed, allowing a higher event rate. The data included in this analysis represent the fraction of the 2012 LHC operation for which this strategy was implemented.

Simulated events are used to model both the signal and background processes. Using PYTHIA 8.165 [20], signal samples with varying neutralino masses M ($200 \leq M \leq 1500\ \text{GeV}$) and life-

times τ ($0.1 \leq c\tau \leq 30$ mm) are produced. In these samples, neutralinos are produced in pairs; each neutralino is forced to undergo a three-body decay into top, bottom, and strange (anti-)quarks. Backgrounds arising from SM processes are dominated by multijet and top quark pair ($t\bar{t}$) events. The multijet processes include b quark pair events. Smaller contributions come from single top quark production (single t), vector boson production in association with additional jets (V+jets), diboson production (VV), and top quark pairs with a radiated vector boson ($t\bar{t} + V$). Processes with a single vector boson include virtual photons, W bosons, or Z bosons, while the diboson processes include WW, WZ, and ZZ. Single top events are simulated with POWHEG 1.0 [21–25]; diboson events are simulated with PYTHIA 6.426 [26]; all other backgrounds are simulated using MADGRAPH 5.1 [27]. For all samples, hadronization and showering are done using PYTHIA 6.426 with tune Z2*. The Z2* tune is derived from the Z1 tune [28], which uses the CTEQ5L parton distribution set, whereas Z2* adopts CTEQ6L [29]. The detector response for all simulated samples is modeled using a GEANT4-based simulation [30] of the CMS detector. The effects of additional pp interactions per bunch crossing (“pileup”) are included by overlaying additional simulated minimum-bias events, such that the resulting distribution of the number of interactions matches that observed in the experiment.

4 Event preselection

To ensure that the four-jet trigger efficiency is high and well understood, more stringent criteria are applied offline, requiring at least four jets in the calorimeter with $p_T > 60$ GeV. These jets are reconstructed from calorimeter energy deposits, which are clustered by the anti- k_T algorithm [31, 32] with a distance parameter of 0.5. The trigger efficiency determined using events satisfying a single-muon trigger is $(96.2 \pm 0.2)\%$ for events with four offline jets with $p_T > 60$ GeV. The simulation overestimates this efficiency by a factor of 1.022 ± 0.002 , so, where used, its normalization is corrected by this amount.

Jets considered in the rest of the analysis are those obtained in the full event reconstruction performed using a particle-flow (PF) algorithm [33, 34]. The PF algorithm reconstructs and identifies photons, electrons, muons, and charged and neutral hadrons with an optimized combination of information from the various elements of the CMS detector. Before clustering the PF candidates into jets, charged PF candidates are excluded if they originate from a pp interaction vertex other than the primary vertex, which is the one with the largest scalar $\sum |p_T|^2$. The resulting particles are clustered into jets, again by the anti- k_T algorithm with a distance parameter of 0.5. Jets used in the analysis must satisfy $p_T > 20$ GeV and $|\eta| < 2.5$.

For an event to be selected for further analysis, the scalar sum of the p_T of jets in the event H_T is required to be at least 500 GeV. This requirement has little impact on signal events but is useful for suppressing SM background.

5 Vertex reconstruction, variables, and selection

5.1 Vertex reconstruction

Displaced vertices are reconstructed from tracks in the CMS silicon tracker. These tracks are required to have $p_T > 1$ GeV, at least eight measurements in the tracker including one in the pixel detector, and a transverse impact parameter with respect to the beam axis of at least $100 \mu\text{m}$. The impact parameter requirement favors vertices that are displaced from the primary vertex. The vertex reconstruction algorithm starts by forming seed vertices from all pairs of tracks that

satisfy these requirements. Each vertex is fitted with the Kalman filter approach [35], and a fit is considered successful if it has a χ^2 per degree of freedom (χ^2/dof) that is less than 5. The vertices are then merged iteratively until no pair of vertices shares tracks. Specifically, for each pair of vertices that shares one or more tracks, if the three-dimensional (3D) distance between the vertices is less than 4 times the uncertainty in that distance, a vertex is fit to the tracks from both, and they are replaced by the merged vertex if the fit has $\chi^2/\text{dof} < 5$. Otherwise, each track is assigned to one vertex or the other depending on its 3D impact parameter significance with respect to each of the vertices, as follows:

- if the track is consistent with both vertices (both impact parameters less than 1.5 standard deviations), assign it to the vertex that has more tracks already;
- if the track's impact parameter is greater than 5 standard deviations from either vertex, drop it from that vertex;
- otherwise, assign the track to the vertex to which it has a smaller impact parameter significance.

Each remaining vertex is then refit, and if the fit satisfies the requirement of $\chi^2/\text{dof} < 5$, the old vertex is replaced with the new one; otherwise it is dropped entirely.

This algorithm is similar in many regards to those used to identify (“tag”) b quark jets [13]. Typical b tagging algorithms, however, are optimized for identifying the decay in flight of a particle into a single jet and consequently make requirements that degrade sensitivity to the multijet final states sought here. For example, b tagging algorithms generally require that the tracks assigned to a vertex are approximately aligned with the flight direction from the primary vertex to the decay point, which is inefficient when there are multiple jets in the final state, including some that may be directed at large angles with respect to the flight path. The b tagging algorithms also discard tracks with impact parameters beyond those typical for b quark daughters (>2 mm), thereby significantly reducing the efficiency for finding vertices with large displacements.

5.2 Vertex variables and selection

The vertexing procedure produces multiple vertices per event, only some of which are consistent with the signal. In order to select quality vertices, we impose additional requirements on the vertex and its associated tracks and jets. The requirements for each vertex are:

- at least five tracks;
- at least three tracks with $p_T > 3$ GeV;
- at least one pair of tracks with separation $\Delta R < 0.4$, where $\Delta R = \sqrt{(\Delta\eta)^2 + (\Delta\phi)^2}$, to favor vertices that include multiple tracks from a single jet;
- at least one pair of tracks with $\Delta R > 1.2$ to favor vertices involving multiple jets;
- $\Delta R < 4$ for all pairs of tracks, to suppress wide-angle track coincidences;
- at least one jet that shares one or more tracks with the vertex;
- displacement in x - y of the vertex from the detector origin of less than 25 mm, to suppress vertices from interactions in the beam pipe or detector material;
- uncertainty in the x - y distance of the vertex from the beam axis of less than 25 μm .

In the data, 181 076 events have one vertex satisfying the above requirements, 251 have two of them, and no events have more than two. The candidate sample is composed of two-vertex events.

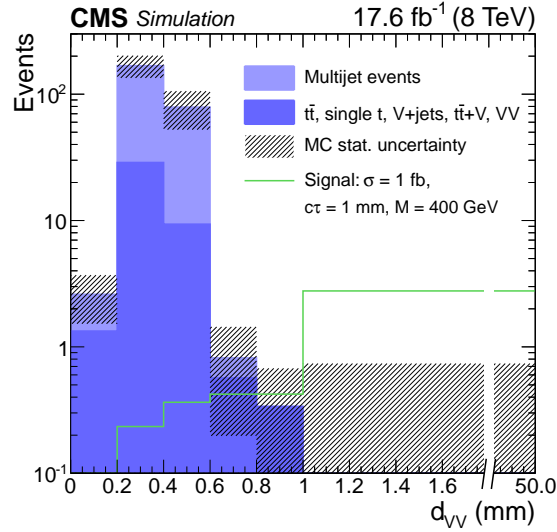


Figure 2: Distribution of the x - y distance between vertices, d_{VV} , for a simulated signal with LSP $c\tau = 1$ mm, $M = 400$ GeV, and production cross section 1 fb, overlaid on simulated background normalized to the observed number of events. All vertex and event selection criteria have been applied. In the last bin where there are no simulated background events, the shaded band represents an approximate 68% confidence level upper limit.

5.3 Signal discrimination in two-vertex events

The signal is extracted from the two-vertex events using the spatial separation between the vertices. In signal events, the two LSPs are emitted approximately back-to-back, leading to large separations. We define the distance between the two vertices in the x - y plane as d_{VV} , and fit this distribution to extract the signal. The fit to the observed d_{VV} distribution is described in Sec. 8.

The signal d_{VV} templates are taken directly from simulation, with a distinct template for each LSP mass M and lifetime τ . In signal simulation, fewer than 10% of events in the candidate sample have more than two selected vertices. For these events, the two vertices with the highest number of tracks are selected for the d_{VV} calculation, and in the case where two vertices have the same number of tracks, the vertex with decay products that have the higher invariant mass is chosen. The mass is reconstructed using the momenta of the associated tracks, assuming that the particles associated with the tracks have the charged pion mass. Figure 2 shows the d_{VV} distribution of an example simulated signal with $c\tau = 1$ mm, $M = 400$ GeV, and production cross section 1 fb, overlaid on the simulated background. The bins in d_{VV} are chosen to be sensitive to the peaking nature of the background at low d_{VV} ; five $200 \mu\text{m}$ bins are used from 0 to 1 mm, then one bin from 1 to 50 mm where the contribution from the long-lived signal dominates.

Figure 3 shows the signal efficiency as a function of LSP mass and lifetime in the region $d_{VV} > 600 \mu\text{m}$, where the background is low. The signal efficiency generally increases as lifetime increases, until the lifetime is so long that decays more often occur beyond our fiducial limit at the beam pipe. The efficiency also generally increases as mass increases, up to approximately 800 GeV where it begins to decrease because of the event selection criteria, particularly the limit on the opening angle between track pairs in a vertex.

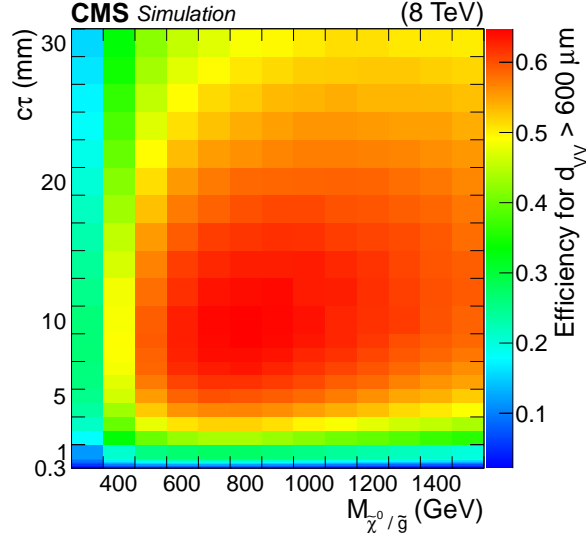


Figure 3: Signal efficiency as a function of neutralino or gluino mass and lifetime. All vertex and event selection criteria have been applied, as well as the requirement $d_{VV} > 600 \mu\text{m}$.

6 Background template

Background vertices arise from poorly measured tracks. These tracks can arise from the same jet, or from several jets in multijet events. Because it is an effect of misreconstruction, two-vertex background events are the coincidence of single background vertices.

Multijet events and $t\bar{t}$ production contribute 85% and 15% of the background in the two-vertex sample, respectively. Other sources of background, such as V+jets and single t events, are negligible. Approximately half of the background events include one or more b quark jets, whose displaced decay daughters combine with misreconstructed tracks to form vertices.

Instead of relying on simulation to reproduce the background, we construct a background template, denoted by d_{VV}^C , from data. Taking advantage of the fact that two-vertex background events can be modeled using the one-vertex events, we define a control sample that consists of the 181 076 events with exactly one vertex. Each value entering the d_{VV}^C template is the distance in the x - y plane between two toy vertices, each determined by a value of the x - y distance from the beam axis to the vertex, denoted by d_{BV} , and a value of the azimuthal angle of the vertex, denoted by ϕ_{BV} .

The two values of d_{BV} are sampled from the distribution of d_{BV} for the one-vertex sample, which is shown in Fig. 4. The observed distribution is in good agreement with the sum of the background contributions from simulation.

The two values of ϕ_{BV} are chosen using information about the jet directions in a one-vertex event. Since background vertices come from misreconstructed tracks, they tend to be located perpendicular to jet momenta. Therefore, we select a jet at random, preferring those with larger p_T because of their higher track multiplicity, and sample a value of ϕ_{BV} from a Gaussian distribution with width 0.4 radians, centered on a direction perpendicular to the jet in the transverse plane. To obtain the second value of ϕ_{BV} , we repeat this procedure using the same one-vertex event, allowing the same jet to be chosen twice.

The vertex reconstruction algorithm merges neighboring vertices. To emulate this behavior in our background template construction procedure, we discard pairs of vertices that are not

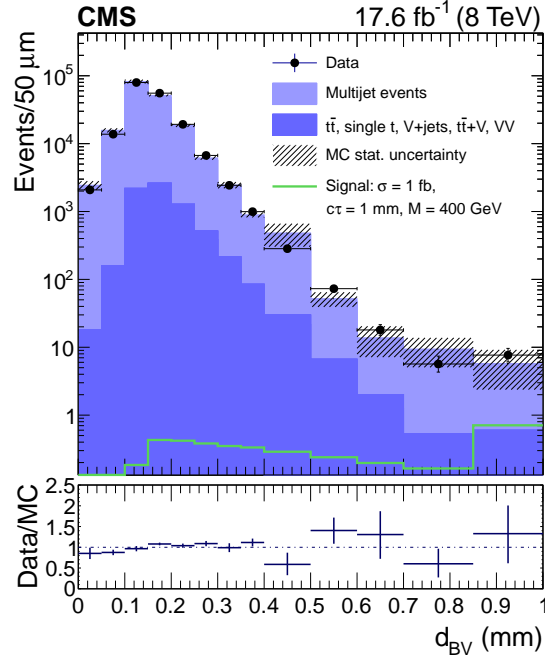


Figure 4: One-vertex events: distribution of the $x-y$ distance from the beam axis to the vertex, d_{BV} , for data, simulated background normalized to data, and a simulated signal with LSP $c\tau = 1$ mm, $M = 400$ GeV, and production cross section 1 fb. Event preselection and vertex selection criteria have been applied. The last bin includes the overflow events.

sufficiently separated. We keep pairs of vertices with a probability parametrized by a Gaussian error function with mean μ_{clear} and width σ_{clear} . The values of μ_{clear} and σ_{clear} , which are related to the position uncertainties of the tracks, are varied in the fit to the observed d_{VV} distribution. The values found in the fit are $\mu_{\text{clear}} = 320 \mu\text{m}$ and $\sigma_{\text{clear}} = 110 \mu\text{m}$.

Figure 5 compares the d_{VV}^C and d_{VV} distributions in simulated events, and shows the variation in d_{VV}^C for values of μ_{clear} and σ_{clear} that are within one standard deviation of the fit values. The agreement is well within the statistical uncertainty. When normalized to the observed number of two-vertex events, the difference in their yields in the region $d_{VV} > 600 \mu\text{m}$ is 0.6 ± 2.6 events.

7 Systematic uncertainties

The signal is extracted from a fit of a weighted sum of the signal and background templates to the observed d_{VV} distribution. For the signal, the simulation provides both the d_{VV} distribution and its normalization, and systematic uncertainties arise from sources such as vertex reconstruction efficiency, track reconstruction, track multiplicity, pileup conditions, the detector alignment, and the jet energies. For the background, for which the template is derived from a control sample, the systematic uncertainties come from effects that could cause a discrepancy between the constructed d_{VV}^C distribution and the nominal d_{VV} distribution.

7.1 Systematic uncertainties related to signal distribution and efficiency

The dominant systematic uncertainty in the signal normalization arises from the difference between the vertexing efficiencies in the simulation and data. This effect is evaluated in an independent study in which artificial signal-like vertices are produced in background events

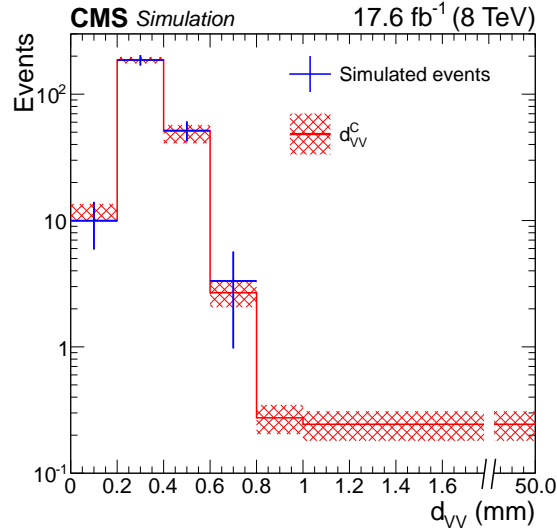


Figure 5: Distribution of the x - y distance between vertices, d_{VV} , for simulated background events (blue crosses), overlaid on the template d_{VV}^C (red line and crosshatches) constructed from simulated one-vertex events. The distributions are normalized to the observed number of two-vertex events. The error bars for the simulated events represent only the statistical uncertainty, while the shaded region for the template is the result of varying μ_{clear} and σ_{clear} within one standard deviation of the values from the fit.

by displacing tracks associated with jets by a known displacement vector, and then applying the vertex reconstruction algorithm. The magnitude of the displacement vector is sampled from an exponential distribution with scale parameter 1 mm, restricted to values between 0.3 and 25 mm, similar to the expected distribution of signal vertices. The direction is calculated from the momentum of the jets in the event, but is smeared to emulate the difference between the flight and momentum directions in simulated signal events due to track inefficiency and unaccounted neutral particles. Events are required to satisfy the preselection requirements described in Sec. 4, and the displaced jets satisfy $p_T > 50$ GeV and $\Delta R < 4$ for all pairs. To estimate the vertexing efficiency, we evaluate the fraction of events in which a vertex satisfying the requirements described in Sec. 5.2 is reconstructed within $50 \mu\text{m}$ of the artificial vertex.

This fraction is evaluated for different numbers of displaced light parton or b quark jets, with the ratio of efficiencies between data and simulation approaching unity for larger numbers of jets, independent of the size of the displacement. The largest disagreement between data and simulation occurs for the case where tracks from two light parton jets are displaced, where the fraction is 70% in simulation and 64% in data, with negligible statistical uncertainty. The ratio of efficiencies between data and simulation gives an 8.6% uncertainty per vertex. For two-vertex events, the uncertainty is 17%.

Additional studies explore the sensitivity of other effects that could alter the signal template. The vertex clustering depends on the number of charged particles in the event, which can vary based on the model of the underlying event used in PYTHIA [36]. The signal templates resulting from the choice of the underlying event model differ by no more than 1% in any bin and the overall efficiency changes by no more than 3%. This 3% is taken as a systematic uncertainty.

To test the sensitivity to a possible misalignment, the signal samples have been reconstructed using several tracker misalignment scenarios corresponding to various “weak modes”: coherent distortions of the tracker geometry left over by the alignment procedure that lead to a

Table 1: Summary of systematic uncertainties in the signal efficiency.

Systematic effect	Uncertainty (%)
Vertex reconstruction	17
Underlying event	3
Tracker misalignment	2
Pileup	1
Jet energy scale/resolution	1
Integrated luminosity	3
Trigger efficiency	1
Overall	18

systematic bias in the track parameters for no penalty in χ^2 of the overall alignment fit [37]. These misalignments change the overall efficiency by no more than 2%, which is taken as a systematic uncertainty.

To study sensitivity to the pileup distribution, we vary the inelastic pp cross section used in the pileup weighting by $\pm 5\%$ [38]. This variation is found to have an effect of less than 1% on the signal efficiency.

The uncertainty in the jet energy scale affects the total energy measured, and could change whether an event passes the jet p_T or H_T selections. This effect is studied by varying the jet energy scale and resolution [18], and is found to change the signal efficiency by less than 1%. A 2.6% uncertainty [39] is associated with the integrated luminosity for the 2012 data set and the derived signal cross section. The uncertainty in the trigger efficiency is less than 1%.

Table 1 summarizes the systematic uncertainties in the signal efficiency. We assume there are no correlations among them, so we add them in quadrature to obtain the overall uncertainty.

7.2 Systematic uncertainties related to background estimate

The d_{VV}^C background template is constructed from a large sample of events with a single vertex. Systematic uncertainties in the d_{VV}^C template are estimated by varying the d_{VV}^C construction method and taking the difference between the d_{VV}^C distributions using the default and alternate methods. The method for constructing d_{VV}^C involves drawing two values of d_{BV} and two values of ϕ_{BV} , with an angle between vertices $\Delta\phi_{VV}$, so the main uncertainties come from effects related to the d_{BV} and $\Delta\phi_{VV}$ distributions.

The production of b quarks in pairs introduces a correlation between the vertex distances in two-vertex events that is not accounted for when single vertices are paired at random. In simulation, events without b quarks have a mean d_{BV} of $\sim 160 \mu\text{m}$, while events with b quarks, which account for 15% of one-vertex events, have a mean d_{BV} of $\sim 190 \mu\text{m}$, without significant dependence on b quark momentum. We quantify this effect by sorting the simulated background events into those with and without b quarks, constructing the d_{VV}^C distributions for each, and then combining them in the proportions 45:55, which is the ratio of b-quark to non-b-quark events in two-vertex background events determined from simulation. The systematic uncertainty is taken to be the difference between the simulated yields obtained with this procedure and the standard one, scaled to the observed two-vertex yield.

The d_{VV}^C construction method discards pairs of vertices that would overlap, consistently leading to a two-vertex angular distribution that peaks at $\pm\pi$ radians. To assess the systematic uncertainty related to assumptions about the angular distribution between vertices, we draw $\Delta\phi_{VV}$ from the angular distribution between vertices in simulated two-vertex background events.

Table 2: Systematic uncertainties in the background yield in each d_{VV} bin arising from construction of the d_{VV}^C template. In the first two rows, shifts are given with their statistical uncertainty. The last row gives the overall systematic uncertainties, assuming no correlations. All yields are normalized to the observed total number of two-vertex events.

Systematic effect	d_{VV} range					
	0.0–0.2 mm	0.2–0.4 mm	0.4–0.6 mm	0.6–0.8 mm	0.8–1.0 mm	1.0–50 mm
d_{BV} correlations	-0.65 ± 0.05	-3.60 ± 1.01	3.59 ± 0.76	0.63 ± 0.18	0.01 ± 0.07	0.01 ± 0.04
$\Delta\phi_{VV}$ modeling	0.74 ± 0.01	1.00 ± 0.00	1.04 ± 0.01	1.18 ± 0.07	-0.01 ± 0.06	-0.01 ± 0.04
d_{BV} sample size	0.05	0.54	0.51	0.17	0.04	0.07
d_{BV} binning	—	—	—	—	0.06	0.09
Overall	1.0	3.9	3.8	1.4	0.1	0.1

This leads to a d_{VV}^C distribution with a more strongly peaked $\Delta\phi_{VV}$ distribution, and provides a conservative estimate of the uncertainty.

The statistical uncertainty from the limited number of one-vertex events that are used to construct the two-vertex distribution is studied using a resampling method. Using the d_{BV} distribution as the parent, we randomly sample ten new d_{BV} pseudodata distributions, and use each to construct a d_{VV}^C distribution. The root-mean-square variation in bin-by-bin yields in the set of distributions gives the statistical uncertainty.

There is a small contribution to the uncertainty in the prediction of d_{VV}^C due to the binning of the d_{BV} parent distribution; moving the d_{BV} tail bin edges around by an amount compatible with the vertex position resolution, $20 \mu\text{m}$, varies the prediction in d_{VV}^C only in the last two bins: by 0.06 events in the 0.8–1.0 mm bin, and by 0.09 events in the 1.0–50 mm bin.

The results of these four studies are summarized in Table 2. In assessing the overall systematic uncertainty in the background template, we add in quadrature the values and their uncertainties, assuming no correlations.

In principle, there can also be uncertainties in the background template due to the effects described in Sec. 7.1. To assess the impact of the underlying event and possible tracker misalignment, we generate five million all-hadronic $t\bar{t}$ events for each scenario, but observe no change in d_{VV}^C larger than 1%. In addition, we vary the inelastic pp cross section used in pileup weighting by $\pm 5\%$, the number of pileup interactions, and the jet energy scale and resolution, and observe effects at the percent-level or less in each case. Since the normalization of the template is a free parameter of the fit, uncertainties such as those in the integrated luminosity, trigger efficiency, and vertex reconstruction efficiency do not enter.

8 Fitting, signal extraction, and statistical interpretation

The distribution of d_{VV} , the separation between vertices in the x - y plane for two-vertex events, is used to discriminate between signal and background, with the signal templates taken directly from the MC simulation and the background template constructed from the observed one-vertex event sample. In the following sections, we describe the fitting and statistical procedures used for the search.

8.1 Fitting procedure

To estimate the signal and background event yields, a binned shape fit is performed using an extended maximum likelihood method. Initially neglecting terms arising from uncertainty in the templates, the log-likelihood function is given by

$$\log \mathcal{L}(n_i|s, b, \boldsymbol{\nu}) = \sum_i [n_i \log a_i(s, b, \boldsymbol{\nu}) - a_i(s, b, \boldsymbol{\nu})]. \quad (1)$$

Here n_i is the number of observed events in bin i ; s and b are the normalizations of the signal and background templates corresponding to the yields; $\boldsymbol{\nu}$ denotes the shape parameters μ_{clear} and σ_{clear} used in the background template construction procedure, as described in Sec. 6; and

$$a_i(s, b, \boldsymbol{\nu}) = sa_i^{(s)} + ba_i^{(b)}(\boldsymbol{\nu}) \quad (2)$$

is the weighted sum of the signal and background frequencies $a_i^{(s)}$ and $a_i^{(b)}$ in bin i .

The only assumed shape uncertainty in the signal templates is that due to the finite MC statistics; the uncertainty is as high as 20% for the lowest lifetime and mass samples, but is generally no more than 1% in any bin for the majority of the templates. For the background templates, a Gaussian uncertainty is assumed in the value of the template in each bin, truncated at zero. To incorporate these uncertainties in the signal and background templates, a procedure similar to that of Barlow and Beeston [40] is followed, modified to allow a bin-by-bin Gaussian uncertainty in the background shape [41]. The final log-likelihood function is then given by

$$\begin{aligned} \log \mathcal{L}(n_i|s, b, \boldsymbol{\nu}, A_i^{(s)}, A_i^{(b)}) &= \sum_i n_i \log A_i - A_i \\ &+ \sum_i M a_i^{(s)} \log M A_i^{(s)} - M A_i^{(s)} \\ &+ \sum_i -\frac{1}{2} \left(\frac{a_i^{(b)} - A_i^{(b)}}{\sigma_i^{(b)}} \right)^2, \quad (3) \end{aligned}$$

with $A_i = sA_i^{(s)} + bA_i^{(b)}$. The $A_i^{(s)}$ and $A_i^{(b)}$ replace the $a_i^{(s)}$ and $a_i^{(b)}$ from above in the shape fit to the data, and are allowed to vary as either Poisson ($A_i^{(s)}$) or Gaussian ($A_i^{(b)}$) distributed parameters. The quantity M is the number of events from the MC signal sample that produced the $a_i^{(s)}$ estimates, and $\sigma_i^{(b)}$ are the widths of the Gaussian distributions taken to be the relative sizes of the uncertainties listed in Table 2. The modified Barlow-Beeston procedure finds the $A_i^{(s)}$ and $A_i^{(b)}$ that maximize $\log \mathcal{L}$ given $(s, b, \boldsymbol{\nu})$; the difference here is that the $A_i^{(b)}$ are Gaussian distributed parameters.

The likelihood function is only weakly dependent on the background shape parameters $\boldsymbol{\nu}$, and when signal is injected, the best fit values $\hat{\boldsymbol{\nu}}$ agree well with the background-only values. The fit is well behaved: for most signal templates, in pseudo-experiments where the true signal and background strengths are known, the distribution of the fitted yields for s and b have means consistent with those input, and the widths of the distributions as measured by their root-mean-square are consistent with the uncertainties in the fits. For the signal templates with low lifetimes, however, the signal yield is biased downward when an injected signal is present. This is due to the background shape being allowed to vary upward at high d_{VV} within the uncertainties assigned. When no injected signal is present, there is a bias toward obtaining $s > 0$ when fitting using templates with $c\tau < 300 \mu\text{m}$. Therefore, we only consider signals with $c\tau \geq 300 \mu\text{m}$ in the fit and the search.

8.2 Statistical analysis

The test statistic q used to quantify any excess of signal events over the expected background is given by a profile likelihood ratio [42]:

$$q = \log \frac{\max_{s \geq 0, b \geq 0} \mathcal{L}(n_i | s, b, \hat{\nu}, \hat{A}_i^{(s)}, \hat{A}_i^{(b)})}{\max_{b \geq 0} \mathcal{L}(n_i | s = 0, b, \hat{\nu}, \hat{A}_i^{(s)}, \hat{A}_i^{(b)})}, \quad (4)$$

where for each value of s and b the nuisance parameters $\hat{A}_i^{(s)}$, $\hat{A}_i^{(b)}$, and $\hat{\nu}$ are found that maximize the relevant likelihood. The probability under the background-only hypothesis, p_0 , to obtain a value of the test statistic at least as large as that observed, q_{obs} , is estimated as the fraction of 10 000 pseudo-experiments with $q \geq q_{\text{obs}}$. This is referred to as the p -value for a particular signal hypothesis. The pseudo-experiments are generated using the background d_{VV}^{C} distribution corresponding to the background-only $\hat{\nu}$, and background count b drawn from a Poisson distribution with mean equal to n , the number of events in the data. The nuisance parameters ν , $A_i^{(s)}$, and $A_i^{(b)}$ are drawn from their corresponding Poisson or Gaussian distributions in each pseudo-experiment.

We obtain limits on the signal yield, which can be converted into limits on the product of the cross section for neutralino or gluino pair production and the square of the branching fraction for decay via the channel under study, denoted by $\sigma \mathcal{B}^2$. To obtain limits on $\sigma \mathcal{B}^2$, for a given number of signal events s_0 , we calculate the probability for the null hypothesis of $s = s_0$ versus the alternative that $s < s_0$ denoted by p_{s_0} . We do this in practice by generating 10 000 pseudo-experiments with s drawn from a Poisson distribution with mean s_0 , and b drawn from a Poisson distribution with mean $n - s_0$. The background shape d_{VV}^{C} is taken from the ν from the original fit and signal shape corresponding to the signal hypothesis in question, with $A_i^{(b)}$ from their Gaussian distributions. The null hypothesis probability p_{s_0} is then the fraction of pseudo-experiments where $q \geq q(s_0)$. We protect against downward fluctuations in the data by using the CL_s criterion [43, 44], defining the statistic as

$$\text{CL}_s = \frac{p_{s_0}}{1 - p_0}. \quad (5)$$

The 95% confidence level (CL) upper limit on s is then the biggest s_0 for which CL_s is still greater than 0.05.

The limit on the signal yield is converted to a limit on $\sigma \mathcal{B}^2$ using the efficiencies calculated from simulation and the integrated luminosity of the data sample, 17.6 fb^{-1} . We include the effect of the estimated 18% signal efficiency uncertainty by varying the cross section in each pseudo-experiment by the value sampled from a log-normal density with location parameter 1 and scale parameter 0.18.

8.3 Results of the fit

The result of the fit to data is shown in Fig. 6, for the LSP $c\tau = 1 \text{ mm}$, $M = 400 \text{ GeV}$ signal template. The observed counts in each bin, along with the predictions from the background-only fit and the related uncertainties, are listed in Table 3. There is a small excess of events with $0.6 < d_{\text{VV}} < 50 \text{ mm}$: 7 in the data, while the background-only fit predicts 4.1 ± 1.4 , where the uncertainty is the overall systematic uncertainty discussed in Sec. 7. In the signal+background fits, a typical value for the signal yield is 1.7 ± 1.9 , obtained with the $c\tau = 1 \text{ mm}$, $M = 400 \text{ GeV}$ signal hypothesis. The associated p -value obtained from pseudo-experiments is in the range

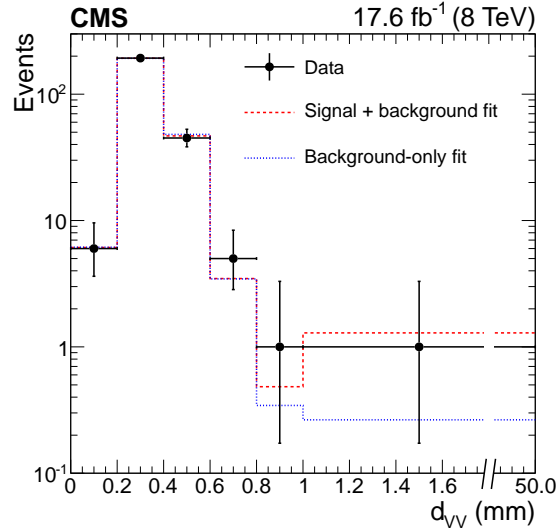


Figure 6: The observed distribution of the x - y distance between the vertices, d_{VV} , shown as points with error bars. Superimposed are the results of the fits with the background-only (blue dotted lines) and signal+background (red dashed lines) hypotheses, using the signal template corresponding to LSP $c\tau = 1$ mm, $M = 400$ GeV.

Table 3: Observed and expected background event yields in each bin. The uncertainty is the sum in quadrature of the statistical and systematic uncertainties.

Bin i	d_{VV} range	Observed n_i	Expected event yield
1	0.0–0.2 mm	6	6.2 ± 1.0
2	0.2–0.4 mm	193	192.6 ± 3.9
3	0.4–0.6 mm	45	48.1 ± 3.8
4	0.6–0.8 mm	5	3.5 ± 1.4
5	0.8–1.0 mm	1	0.3 ± 0.1
6	1.0–50 mm	1	0.3 ± 0.1

0.05–0.14 for signals with $0.3 \leq c\tau \leq 30$ mm, with the larger p -values coming from those with longer lifetimes.

8.4 Upper limits on signal cross section

Figure 7 shows the observed 95% CL upper limits on $\sigma\mathcal{B}^2$. As an example, for a neutralino with mass of 400 GeV and $c\tau$ of 10 mm, the observed 95% CL upper limit on $\sigma\mathcal{B}^2$ is 0.6 fb.

Exclusion curves are overlaid, assuming the gluino pair production cross section [45–49]. In the context of the MFV model that we are studying, either a neutralino or a gluino LSP can decay into the final state targeted in the search.

The scan in $c\tau$ is in steps of $100 \mu\text{m}$ from $300 \mu\text{m}$ to 1 mm, then in 1 mm steps up to 10 mm, and in 2 mm steps to 30 mm; the mass points are spaced by 100 GeV. The exclusion curves are produced by linear interpolation of the limit scan, which identifies the set of points for which the interpolated upper limit is less than the gluino pair production cross section (the neutralino pair production cross section is expected to be much smaller).

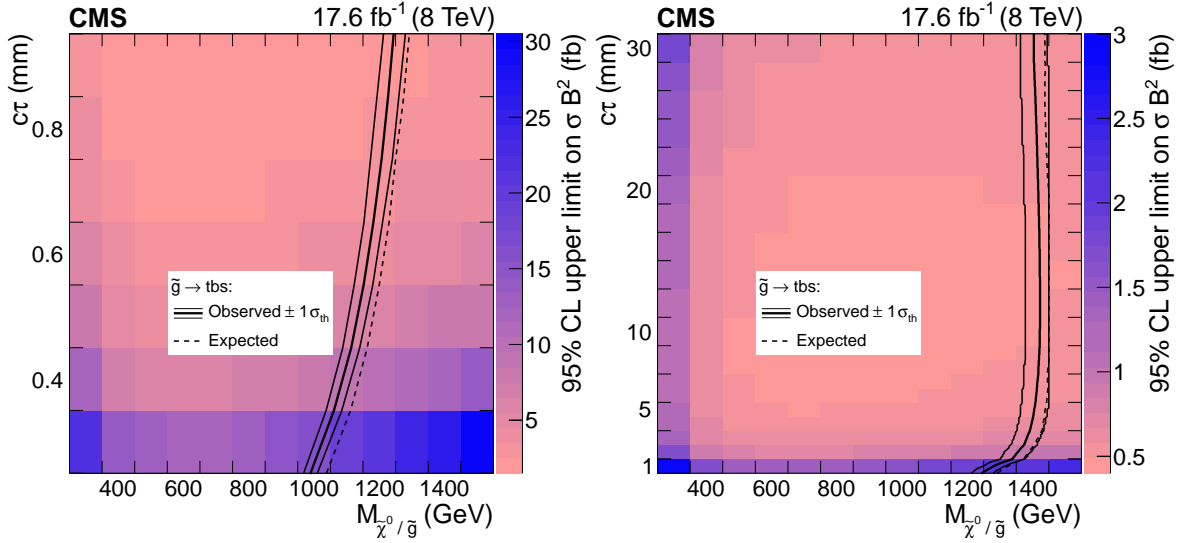


Figure 7: Observed 95% CL upper limits on cross section times branching fraction squared, with overlaid curves assuming gluino pair production cross section, for both observed (solid), with ± 1 standard deviation theoretical uncertainties, and expected (dashed) limits. The search excludes masses to the left of the curve. The left plot spans $c\tau$ from 300 through 900 μm , while the right plot ranges from 1 to 30 mm.

9 Extending the search to other signal models

The search for displaced vertices applies to other types of long-lived particles decaying to multiple jets. Here we present a generator-level selection that can be used to reinterpret the results of our analysis. For signal models in which there are two well-separated displaced vertices, this generator-level selection approximately replicates the reconstruction-level efficiency. The selection is based on the displacements of the long-lived particles, and the momenta and angular distributions of their daughter particles, which are taken to be u , d , s , c , and b quarks; electrons; and muons. The daughter particles are said to be “accepted” if they satisfy $p_T > 20 \text{ GeV}$ and $|\eta| < 2.5$, and “displaced” if their transverse impact parameter with respect to the origin is at least $100 \mu\text{m}$. The criteria of the generator-level selection are:

- at least four accepted quarks with $p_T > 60 \text{ GeV}$;
- H_T of accepted quarks $> 500 \text{ GeV}$;
- for each vertex:
 - x - y distance from beam axis $< 25 \text{ mm}$;
 - at least one pair of accepted displaced daughter particles with $\Delta R > 1.2$;
 - $\Delta R < 4$ for all pairs of accepted displaced daughter particles;
 - at least one accepted displaced daughter quark;
 - $\sum p_T$ of accepted displaced daughter particles $> 200 \text{ GeV}$;
- x - y distance between vertices $> 600 \mu\text{m}$.

In the region with $d_{VV} > 600 \mu\text{m}$, the background level is well determined and is insensitive to fit parameters. Use of this generator-level selection replicates the reconstruction-level efficiency with an accuracy of 20% or better for a selection of models for which the signal efficiency is high ($> 10\%$). The selection may underestimate the trigger efficiency because it does not take into account effects such as initial- and final-state radiation, and may overestimate the efficiency

for reconstructing vertices with b quark secondaries, since the b quark lifetime can impede the association of their decay products with the reconstructed vertices.

10 Summary

A search for R -parity violating SUSY in which long-lived neutralinos or gluinos decay into multijet final states was performed using proton-proton collision events collected with the CMS detector at $\sqrt{s} = 8$ TeV in 2012. The data sample corresponded to an integrated luminosity of 17.6 fb^{-1} , and was collected requiring the presence of at least four jets. No excess above the prediction from standard model processes was observed, and at 95% confidence level, the data excluded cross section times branching fraction squared above approximately 1 fb for neutralinos or gluinos with mass between 400 and 1500 GeV and $c\tau$ between 1 and 30 mm. Assuming gluino pair production cross sections, gluino masses below 1 and 1.3 TeV were excluded for mean proper decay lengths of $300 \mu\text{m}$ and 1 mm, respectively, and below 1.4 TeV for the range 2–30 mm. While the search specifically addressed R -parity violating SUSY, the results were relevant to other massive particles that decay to two or more jets. These are the most restrictive bounds to date on the production and decay of pairs of such massive particles with intermediate lifetimes.

Acknowledgments

We congratulate our colleagues in the CERN accelerator departments for the excellent performance of the LHC and thank the technical and administrative staffs at CERN and at other CMS institutes for their contributions to the success of the CMS effort. In addition, we gratefully acknowledge the computing centers and personnel of the Worldwide LHC Computing Grid for delivering so effectively the computing infrastructure essential to our analyses. Finally, we acknowledge the enduring support for the construction and operation of the LHC and the CMS detector provided by the following funding agencies: BMWFW and FWF (Austria); FNRS and FWO (Belgium); CNPq, CAPES, FAPERJ, and FAPESP (Brazil); MES (Bulgaria); CERN; CAS, MoST, and NSFC (China); COLCIENCIAS (Colombia); MSES and CSF (Croatia); RPF (Cyprus); SENESCYT (Ecuador); MoER, ERC IUT, and ERDF (Estonia); Academy of Finland, MEC, and HIP (Finland); CEA and CNRS/IN2P3 (France); BMBF, DFG, and HGF (Germany); GSRT (Greece); OTKA and NIH (Hungary); DAE and DST (India); IPM (Iran); SFI (Ireland); INFN (Italy); MSIP and NRF (Republic of Korea); LAS (Lithuania); MOE and UM (Malaysia); BUAP, CINVESTAV, CONACYT, LNS, SEP, and UASLP-FAI (Mexico); MBIE (New Zealand); PAEC (Pakistan); MSHE and NSC (Poland); FCT (Portugal); JINR (Dubna); MON, RosAtom, RAS, and RFBR (Russia); MESTD (Serbia); SEIDI and CPAN (Spain); Swiss Funding Agencies (Switzerland); MST (Taipei); ThEPCenter, IPST, STAR, and NSTDA (Thailand); TUBITAK and TAEK (Turkey); NASU and SFFR (Ukraine); STFC (United Kingdom); DOE and NSF (USA).

Individuals have received support from the Marie-Curie program and the European Research Council and EPLANET (European Union); the Leventis Foundation; the A. P. Sloan Foundation; the Alexander von Humboldt Foundation; the Belgian Federal Science Policy Office; the Fonds pour la Formation à la Recherche dans l'Industrie et dans l'Agriculture (FRIA-Belgium); the Agentschap voor Innovatie door Wetenschap en Technologie (IWT-Belgium); the Ministry of Education, Youth and Sports (MEYS) of the Czech Republic; the Council of Science and Industrial Research, India; the HOMING PLUS program of the Foundation for Polish Science, cofinanced from European Union, Regional Development Fund, the Mobility Plus program of the Ministry of Science and Higher Education, the National Science Center (Poland), contracts

Harmonia 2014/14/M/ST2/00428, Opus 2013/11/B/ST2/04202, 2014/13/B/ST2/02543 and 2014/15/B/ST2/03998, Sonata-bis 2012/07/E/ST2/01406; the Thalys and Aristeia programs cofinanced by EU-ESF and the Greek NSRF; the National Priorities Research Program by Qatar National Research Fund; the Programa Clarín-COFUND del Principado de Asturias; the Rachadapisek Sompot Fund for Postdoctoral Fellowship, Chulalongkorn University and the Chulalongkorn Academic into Its 2nd Century Project Advancement Project (Thailand); and the Welch Foundation, contract C-1845.

References

- [1] H. P. Nilles, “Supersymmetry, supergravity and particle physics”, *Phys. Rept.* **110** (1984) 1, doi:10.1016/0370-1573(84)90008-5.
- [2] H. E. Haber and G. L. Kane, “The search for supersymmetry: probing physics beyond the standard model”, *Phys. Rept.* **117** (1985) 75, doi:10.1016/0370-1573(85)90051-1.
- [3] G. R. Farrar and P. Fayet, “Phenomenology of the production, decay, and detection of new hadronic states associated with supersymmetry”, *Phys. Lett. B* **76** (1978) 575, doi:10.1016/0370-2693(78)90858-4.
- [4] S. Weinberg, “Supersymmetry at ordinary energies. Masses and conservation laws”, *Phys. Rev. D* **26** (1982) 287, doi:10.1103/PhysRevD.26.287.
- [5] R. Barbier et al., “ R -parity violating supersymmetry”, *Phys. Rept.* **420** (2005) 1, doi:10.1016/j.physrep.2005.08.006, arXiv:hep-ph/0406039.
- [6] ATLAS Collaboration, “Search for pair production of massive particles decaying into three quarks with the ATLAS detector in $\sqrt{s} = 7$ TeV pp collisions at the LHC”, *JHEP* **12** (2012) 086, doi:10.1007/JHEP12(2012)086, arXiv:1210.4813.
- [7] CMS Collaboration, “Searches for light- and heavy-flavour three-jet resonances in pp collisions at $\sqrt{s} = 8$ TeV”, *Phys. Lett. B* **730** (2014) 193, doi:10.1016/j.physletb.2014.01.049, arXiv:1311.1799.
- [8] ATLAS Collaboration, “Search for massive supersymmetric particles decaying to many jets using the ATLAS detector in pp collisions at $\sqrt{s} = 8$ TeV”, *Phys. Rev. D* **91** (2015) 112016, doi:10.1103/PhysRevD.91.112016, arXiv:1502.05686.
- [9] ATLAS Collaboration, “Search for supersymmetry in events with four or more leptons in $\sqrt{s} = 8$ TeV pp collisions with the ATLAS detector”, *Phys. Rev. D* **90** (2014) 052001, doi:10.1103/PhysRevD.90.052001, arXiv:1405.5086.
- [10] CMS Collaboration, “Searches for R -parity violating supersymmetry in pp collisions at $\sqrt{s} = 8$ TeV in final states with 0–4 leptons”, (2016). arXiv:1606.08076. Submitted for publication in Phys. Rev. D.
- [11] E. Nikolidakis and C. Smith, “Minimal flavor violation, seesaw mechanism, and R -parity”, *Phys. Rev. D* **77** (2008) 015021, doi:10.1103/PhysRevD.77.015021, arXiv:0710.3129.
- [12] C. Csáki, Y. Grossman, and B. Heidenreich, “Minimal flavor violation supersymmetry: a natural theory for R -parity violation”, *Phys. Rev. D* **85** (2012) 095009, doi:10.1103/PhysRevD.85.095009, arXiv:1111.1239.

- [13] CMS Collaboration, "Identification of b-quark jets with the CMS experiment", *J. Instrum.* **8** (2013) P04013, doi:10.1088/1748-0221/8/04/P04013.
- [14] CMS Collaboration, "Search for long-lived neutral particles decaying to quark-antiquark pairs in proton-proton collisions at $\sqrt{s} = 8$ TeV", *Phys. Rev. D* **91** (2015) 012007, doi:10.1103/PhysRevD.91.012007.
- [15] ATLAS Collaboration, "Search for massive, long-lived particles using multitrack displaced vertices or displaced lepton pairs in pp collisions at $\sqrt{s} = 8$ TeV with the ATLAS detector", *Phys. Rev. D* **92** (2015) 072004, doi:10.1103/PhysRevD.92.072004, arXiv:1504.05162.
- [16] CMS Collaboration, "The CMS experiment at the CERN LHC", *J. Instrum.* **3** (2008) S08004, doi:10.1088/1748-0221/3/08/S08004.
- [17] CMS Collaboration, "Description and performance of track and primary-vertex reconstruction with the CMS tracker", *J. Instrum.* **9** (2014) P10009, doi:10.1088/1748-0221/9/10/P10009.
- [18] CMS Collaboration, "Determination of jet energy calibration and transverse momentum resolution in CMS", *J. Instrum.* **6** (2011) P11002, doi:10.1088/1748-0221/6/11/P11002.
- [19] CMS Collaboration, "Data parking and data scouting at the CMS experiment", CMS Detector Performance Note CMS-DP-2012-022, 2012.
- [20] T. Sjöstrand, S. Mrenna, and P. Skands, "A brief introduction to PYTHIA 8.1", *Comput. Phys. Commun.* **178** (2008) 852, doi:10.1016/j.cpc.2008.01.036, arXiv:0710.3820.
- [21] P. Nason, "A new method for combining NLO QCD with shower Monte Carlo algorithms", *JHEP* **11** (2004) 040, doi:10.1088/1126-6708/2004/11/040, arXiv:hep-ph/0409146.
- [22] S. Frixione, P. Nason, and C. Oleari, "Matching NLO QCD computations with parton shower simulations: the POWHEG method", *JHEP* **11** (2007) 070, doi:10.1088/1126-6708/2007/11/070, arXiv:0709.2092.
- [23] S. Alioli, P. Nason, C. Oleari, and E. Re, "A general framework for implementing NLO calculations in shower Monte Carlo programs: the POWHEG BOX", *JHEP* **06** (2010) 043, doi:10.1007/JHEP06(2010)043, arXiv:1002.2581.
- [24] S. Alioli, P. Nason, C. Oleari, and E. Re, "NLO single-top production matched with shower in POWHEG: s - and t -channel contributions", *JHEP* **09** (2009) 111, doi:10.1088/1126-6708/2009/09/111, arXiv:0907.4076.
- [25] E. Re, "Single-top Wt -channel production matched with parton showers using the POWHEG method", *Eur. Phys. J. C* **71** (2011) 1547, doi:10.1140/epjc/s10052-011-1547-z, arXiv:1009.2450.
- [26] T. Sjöstrand, S. Mrenna, and P. Skands, "PYTHIA 6.4 physics and manual", *JHEP* **05** (2006) 026, doi:10.1088/1126-6708/2006/05/026, arXiv:hep-ph/0603175.
- [27] J. Alwall et al., "MadGraph 5: going beyond", *JHEP* **06** (2011) 128, doi:10.1007/JHEP06(2011)128, arXiv:1106.0522.

- [28] R. Field, “Early LHC underlying event data—findings and surprises”, in *Hadron Collider Physics. Proceedings, 22nd Conference, HCP 2010, Toronto, Canada, August 23-27, 2010*. 2010. arXiv:1010.3558.
- [29] J. Pumplin et al., “New generation of parton distributions with uncertainties from global QCD analysis”, *JHEP* **07** (2002) 012, doi:10.1088/1126-6708/2002/07/012, arXiv:hep-ph/0201195.
- [30] GEANT4 Collaboration, “GEANT4—a simulation toolkit”, *Nucl. Instrum. Meth. A* **506** (2003) 250, doi:10.1016/S0168-9002(03)01368-8.
- [31] M. Cacciari, G. P. Salam, and G. Soyez, “The anti- k_t jet clustering algorithm”, *JHEP* **04** (2008) 063, doi:10.1088/1126-6708/2008/04/063, arXiv:0802.1189.
- [32] M. Cacciari, G. P. Salam, and G. Soyez, “FastJet user manual”, *Eur. Phys. J. C* **72** (2012) 1896, doi:10.1140/epjc/s10052-012-1896-2, arXiv:1111.6097.
- [33] CMS Collaboration, “Particle-flow event reconstruction in CMS and performance for jets, taus, and E_T^{miss} ”, CMS Physics Analysis Summary CMS-PAS-PFT-09-001, 2009.
- [34] CMS Collaboration, “Commissioning of the particle-flow event reconstruction with the first LHC collisions recorded in the CMS detector”, CMS Physics Analysis Summary CMS-PAS-PFT-10-001, 2010.
- [35] R. Frühwirth, “Application of Kalman filtering to track and vertex fitting”, *Nucl. Instrum. Meth. A* **262** (1987) 444, doi:10.1016/0168-9002(87)90887-4.
- [36] CMS Collaboration, “Event generator tunes obtained from underlying event and multiparton scattering measurements”, *Eur. Phys. J. C* **76** (2016) 155, doi:10.1140/epjc/s10052-016-3988-x, arXiv:1512.00815.
- [37] CMS Collaboration, “Alignment of the CMS tracker with LHC and cosmic ray data”, *J. Instrum.* **9** (2014) P06009, doi:10.1088/1748-0221/9/06/P06009.
- [38] CMS Collaboration, “Measurement of the inelastic proton-proton cross section at $\sqrt{s} = 7$ TeV”, *Phys. Lett. B* **722** (2013) 5, doi:10.1016/j.physletb.2013.03.024.
- [39] CMS Collaboration, “CMS luminosity based on pixel cluster counting—summer 2013 update”, CMS Physics Analysis Summary CMS-PAS-LUM-13-001, 2013.
- [40] R. Barlow and C. Beeston, “Fitting using finite Monte Carlo samples”, *Comput. Phys. Commun.* **77** (1993) 219, doi:10.1016/0010-4655(93)90005-W.
- [41] J. S. Conway, “Incorporating nuisance parameters in likelihoods for multisource spectra”, in *Proceedings, PHYSTAT 2011 Workshop on Statistical Issues Related to Discovery Claims in Search Experiments and Unfolding, CERN, Geneva, Switzerland 17-20 January 2011*. 2011. arXiv:1103.0354. doi:10.5170/CERN-2011-006.115.
- [42] W. A. Rolke, A. M. López, and J. Conrad, “Limits and confidence intervals in the presence of nuisance parameters”, *Nucl. Instrum. Meth. A* **551** (2005) 493, doi:10.1016/j.nima.2005.05.068, arXiv:physics/0403059.
- [43] A. L. Read, “Presentation of search results: the CL_S technique”, *J. Phys. G* **28** (2002) 2693, doi:10.1088/0954-3899/28/10/313.

- [44] T. Junk, "Confidence level computation for combining searches with small statistics", *Nucl. Instrum. Meth. A* **434** (1999) 435, doi:10.1016/S0168-9002(99)00498-2, arXiv:hep-ex/9902006.
- [45] W. Beenakker, R. Höpker, M. Spira, and P. M. Zerwas, "Squark and gluino production at hadron colliders", *Nucl. Phys. B* **492** (1997) 51, doi:10.1016/S0550-3213(97)80027-2, arXiv:hep-ph/9610490.
- [46] A. Kulesza and L. Motyka, "Threshold Resummation for Squark-Antisquark and Gluino-Pair Production at the LHC", *Phys. Rev. Lett.* **102** (2009) 111802, doi:10.1103/PhysRevLett.102.111802, arXiv:0807.2405.
- [47] A. Kulesza and L. Motyka, "Soft gluon resummation for the production of gluino-gluino and squark-antisquark pairs at the LHC", *Phys. Rev. D* **80** (2009) 095004, doi:10.1103/PhysRevD.80.095004, arXiv:0905.4749.
- [48] W. Beenakker et al., "Soft-gluon resummation for squark and gluino hadroproduction", *JHEP* **12** (2009) 041, doi:10.1088/1126-6708/2009/12/041, arXiv:0909.4418.
- [49] W. Beenakker et al., "Squark and gluino hadroproduction", *Int. J. Mod. Phys. A* **26** (2011) 2637, doi:10.1142/S0217751X11053560, arXiv:1105.1110.

A The CMS Collaboration

Yerevan Physics Institute, Yerevan, Armenia

V. Khachatryan, A.M. Sirunyan, A. Tumasyan

Institut für Hochenergiephysik, Wien, Austria

W. Adam, E. Asilar, T. Bergauer, J. Brandstetter, E. Brondolin, M. Dragicevic, J. Erö, M. Flechl, M. Friedl, R. Frühwirth¹, V.M. Ghete, C. Hartl, N. Hörmann, J. Hrubec, M. Jeitler¹, A. König, I. Krätschmer, D. Liko, T. Matsushita, I. Mikulec, D. Rabadý, N. Rad, B. Rahbaran, H. Rohringer, J. Schieck¹, J. Strauss, W. Treberer-Treberspurg, W. Waltenberger, C.-E. Wulz¹

National Centre for Particle and High Energy Physics, Minsk, Belarus

V. Mossolov, N. Shumeiko, J. Suarez Gonzalez

Universiteit Antwerpen, Antwerpen, Belgium

S. Alderweireldt, E.A. De Wolf, X. Janssen, J. Lauwers, M. Van De Klundert, H. Van Haevermaet, P. Van Mechelen, N. Van Remortel, A. Van Spilbeeck

Vrije Universiteit Brussel, Brussel, Belgium

S. Abu Zeid, F. Blekman, J. D'Hondt, N. Daci, I. De Bruyn, K. Deroover, N. Heracleous, S. Lowette, S. Moortgat, L. Moreels, A. Olbrechts, Q. Python, S. Tavernier, W. Van Doninck, P. Van Mulders, I. Van Parijs

Université Libre de Bruxelles, Bruxelles, Belgium

H. Brun, C. Caillol, B. Clerbaux, G. De Lentdecker, H. Delannoy, G. Fasanella, L. Favart, R. Goldouzian, A. Grebenyuk, G. Karapostoli, T. Lenzi, A. Léonard, J. Luetic, T. Maerschalk, A. Marinov, A. Randle-conde, T. Seva, C. Vander Velde, P. Vanlaer, R. Yonamine, F. Zenoni, F. Zhang²

Ghent University, Ghent, Belgium

A. Cimmino, T. Cornelis, D. Dobur, A. Fagot, G. Garcia, M. Gul, D. Poyraz, S. Salva, R. Schöfbeck, M. Tytgat, W. Van Driessche, E. Yazgan, N. Zaganidis

Université Catholique de Louvain, Louvain-la-Neuve, Belgium

H. Bakhshiansohi, C. Beluffi³, O. Bondu, S. Brochet, G. Bruno, A. Caudron, S. De Visscher, C. Delaere, M. Delcourt, L. Forthomme, B. Francois, A. Giammanco, A. Jafari, P. Jez, M. Komm, V. Lemaître, A. Magitteri, A. Mertens, M. Musich, C. Nuttens, K. Piotrkowski, L. Quertenmont, M. Selvaggi, M. Vidal Marono, S. Wertz

Université de Mons, Mons, Belgium

N. Bely

Centro Brasileiro de Pesquisas Físicas, Rio de Janeiro, Brazil

W.L. Aldá Júnior, F.L. Alves, G.A. Alves, L. Brito, C. Hensel, A. Moraes, M.E. Pol, P. Rebello Teles

Universidade do Estado do Rio de Janeiro, Rio de Janeiro, Brazil

E. Belchior Batista Das Chagas, W. Carvalho, J. Chinellato⁴, A. Custódio, E.M. Da Costa, G.G. Da Silveira, D. De Jesus Damiao, C. De Oliveira Martins, S. Fonseca De Souza, L.M. Huertas Guativa, H. Malbouisson, D. Matos Figueiredo, C. Mora Herrera, L. Mundim, H. Nogima, W.L. Prado Da Silva, A. Santoro, A. Sznajder, E.J. Tonelli Manganote⁴, A. Vilela Pereira

Universidade Estadual Paulista ^a, Universidade Federal do ABC ^b, São Paulo, Brazil

S. Ahuja^a, C.A. Bernardes^b, S. Dogra^a, T.R. Fernandez Perez Tomei^a, E.M. Gregores^b,

P.G. Mercadante^b, C.S. Moon^a, S.F. Novaes^a, Sandra S. Padula^a, D. Romero Abad^b, J.C. Ruiz Vargas

Institute for Nuclear Research and Nuclear Energy, Sofia, Bulgaria

A. Aleksandrov, R. Hadjiiska, P. Iaydjiev, M. Rodozov, S. Stoykova, G. Sultanov, M. Vutova

University of Sofia, Sofia, Bulgaria

A. Dimitrov, I. Glushkov, L. Litov, B. Pavlov, P. Petkov

Beihang University, Beijing, China

W. Fang⁵

Institute of High Energy Physics, Beijing, China

M. Ahmad, J.G. Bian, G.M. Chen, H.S. Chen, M. Chen, Y. Chen⁶, T. Cheng, C.H. Jiang, D. Leggat, Z. Liu, F. Romeo, S.M. Shaheen, A. Spiezia, J. Tao, C. Wang, Z. Wang, H. Zhang, J. Zhao

State Key Laboratory of Nuclear Physics and Technology, Peking University, Beijing, China

Y. Ban, G. Chen, Q. Li, S. Liu, Y. Mao, S.J. Qian, D. Wang, Z. Xu

Universidad de Los Andes, Bogota, Colombia

C. Avila, A. Cabrera, L.F. Chaparro Sierra, C. Florez, J.P. Gomez, C.F. González Hernández, J.D. Ruiz Alvarez, J.C. Sanabria

University of Split, Faculty of Electrical Engineering, Mechanical Engineering and Naval Architecture, Split, Croatia

N. Godinovic, D. Lelas, I. Puljak, P.M. Ribeiro Cipriano

University of Split, Faculty of Science, Split, Croatia

Z. Antunovic, M. Kovac

Institute Rudjer Boskovic, Zagreb, Croatia

V. Brigljevic, D. Ferencek, K. Kadija, S. Micanovic, L. Sudic, T. Susa

University of Cyprus, Nicosia, Cyprus

A. Attikis, G. Mavromanolakis, J. Mousa, C. Nicolaou, F. Ptochos, P.A. Razis, H. Rykaczewski

Charles University, Prague, Czech Republic

M. Finger⁷, M. Finger Jr.⁷

Universidad San Francisco de Quito, Quito, Ecuador

E. Carrera Jarrin

Academy of Scientific Research and Technology of the Arab Republic of Egypt, Egyptian Network of High Energy Physics, Cairo, Egypt

A. Ellithi Kamel⁸, M.A. Mahmoud^{9,10}, A. Radi^{10,11}

National Institute of Chemical Physics and Biophysics, Tallinn, Estonia

B. Calpas, M. Kadastik, M. Murumaa, L. Perrini, M. Raidal, A. Tiko, C. Veelken

Department of Physics, University of Helsinki, Helsinki, Finland

P. Eerola, J. Pekkanen, M. Voutilainen

Helsinki Institute of Physics, Helsinki, Finland

J. Härkönen, V. Karimäki, R. Kinnunen, T. Lampén, K. Lassila-Perini, S. Lehti, T. Lindén, P. Luukka, T. Peltola, J. Tuominiemi, E. Tuovinen, L. Wendland

Lappeenranta University of Technology, Lappeenranta, Finland

J. Talvitie, T. Tuuva

IRFU, CEA, Université Paris-Saclay, Gif-sur-Yvette, France

M. Besancon, F. Couderc, M. Dejardin, D. Denegri, B. Fabbro, J.L. Faure, C. Favaro, F. Ferri, S. Ganjour, S. Ghosh, A. Givernaud, P. Gras, G. Hamel de Monchenault, P. Jarry, I. Kucher, E. Locci, M. Machet, J. Malcles, J. Rander, A. Rosowsky, M. Titov, A. Zghiche

Laboratoire Leprince-Ringuet, Ecole Polytechnique, IN2P3-CNRS, Palaiseau, France

A. Abdulsalam, I. Antropov, S. Baffioni, F. Beaudette, P. Busson, L. Cadamuro, E. Chapon, C. Charlot, O. Davignon, R. Granier de Cassagnac, M. Jo, S. Lisniak, P. Miné, M. Nguyen, C. Ochando, G. Ortona, P. Paganini, P. Pigard, S. Regnard, R. Salerno, Y. Sirois, T. Strebler, Y. Yilmaz, A. Zabi

Institut Pluridisciplinaire Hubert Curien, Université de Strasbourg, Université de Haute Alsace Mulhouse, CNRS/IN2P3, Strasbourg, FranceJ.-L. Agram¹², J. Andrea, A. Aubin, D. Bloch, J.-M. Brom, M. Buttignol, E.C. Chabert, N. Chanon, C. Collard, E. Conte¹², X. Coubez, J.-C. Fontaine¹², D. Gelé, U. Goerlach, A.-C. Le Bihan, J.A. Merlin¹³, K. Skovpen, P. Van Hove**Centre de Calcul de l'Institut National de Physique Nucleaire et de Physique des Particules, CNRS/IN2P3, Villeurbanne, France**

S. Gadrat

Université de Lyon, Université Claude Bernard Lyon 1, CNRS-IN2P3, Institut de Physique Nucléaire de Lyon, Villeurbanne, FranceS. Beauceron, C. Bernet, G. Boudoul, E. Bouvier, C.A. Carrillo Montoya, R. Chierici, D. Contardo, B. Courbon, P. Depasse, H. El Mamouni, J. Fan, J. Fay, S. Gascon, M. Gouzevitch, G. Grenier, B. Ille, F. Lagarde, I.B. Laktineh, M. Lethuillier, L. Mirabito, A.L. Pequegnot, S. Perries, A. Popov¹⁴, D. Sabes, V. Sordini, M. Vander Donckt, P. Verdier, S. Viret**Georgian Technical University, Tbilisi, Georgia**T. Toriashvili¹⁵**Tbilisi State University, Tbilisi, Georgia**Z. Tsamalaidze⁷**RWTH Aachen University, I. Physikalisches Institut, Aachen, Germany**C. Autermann, S. Beranek, L. Feld, A. Heister, M.K. Kiesel, K. Klein, M. Lipinski, A. Ostapchuk, M. Preuten, F. Raupach, S. Schael, C. Schomakers, J.F. Schulte, J. Schulz, T. Verlage, H. Weber, V. Zhukov¹⁴**RWTH Aachen University, III. Physikalisches Institut A, Aachen, Germany**

M. Brodski, E. Dietz-Laursonn, D. Duchardt, M. Endres, M. Erdmann, S. Erdweg, T. Esch, R. Fischer, A. Güth, M. Hamer, T. Hebbeker, C. Heidemann, K. Hoepfner, S. Knutzen, M. Merschmeyer, A. Meyer, P. Millet, S. Mukherjee, M. Olschewski, K. Padeken, T. Pook, M. Radziej, H. Reithler, M. Rieger, F. Scheuch, L. Sonnenschein, D. Teyssier, S. Thüer

RWTH Aachen University, III. Physikalisches Institut B, Aachen, GermanyV. Cherepanov, G. Flügge, W. Haj Ahmad, F. Hoehle, B. Kargoll, T. Kress, A. Künsken, J. Lingemann, A. Nehr Korn, A. Nowack, I.M. Nugent, C. Pistone, O. Pooth, A. Stahl¹³**Deutsches Elektronen-Synchrotron, Hamburg, Germany**M. Aldaya Martin, C. Asawatangtrakuldee, K. Beernaert, O. Behnke, U. Behrens, A.A. Bin Anuar, K. Borras¹⁶, A. Campbell, P. Connor, C. Contreras-Campana, F. Costanza, C. Diez

Pardos, G. Dolinska, G. Eckerlin, D. Eckstein, E. Eren, E. Gallo¹⁷, J. Garay Garcia, A. Geiser, A. Gizhko, J.M. Grados Luyando, P. Gunnellini, A. Harb, J. Hauk, M. Hempel¹⁸, H. Jung, A. Kalogeropoulos, O. Karacheban¹⁸, M. Kasemann, J. Keaveney, J. Kieseler, C. Kleinwort, I. Korol, D. Krücker, W. Lange, A. Lelek, J. Leonard, K. Lipka, A. Lobanov, W. Lohmann¹⁸, R. Mankel, I.-A. Melzer-Pellmann, A.B. Meyer, G. Mittag, J. Mnich, A. Mussgiller, E. Ntomari, D. Pitzl, R. Placakyte, A. Raspereza, B. Roland, M.Ö. Sahin, P. Saxena, T. Schoerner-Sadenius, C. Seitz, S. Spannagel, N. Stefaniuk, K.D. Trippkewitz, G.P. Van Onsem, R. Walsh, C. Wissing

University of Hamburg, Hamburg, Germany

V. Blobel, M. Centis Vignali, A.R. Draeger, T. Dreyer, E. Garutti, K. Goebel, D. Gonzalez, J. Haller, M. Hoffmann, A. Junkes, R. Klanner, R. Kogler, N. Kovalchuk, T. Lapsien, T. Lenz, I. Marchesini, D. Marconi, M. Meyer, M. Niedziela, D. Nowatschin, J. Ott, F. Pantaleo¹³, T. Peiffer, A. Perieanu, J. Poehlsen, C. Sander, C. Scharf, P. Schleper, A. Schmidt, S. Schumann, J. Schwandt, H. Stadie, G. Steinbrück, F.M. Stober, M. Stöver, H. Tholen, D. Troendle, E. Usai, L. Vanelderen, A. Vanhoefer, B. Vormwald

Institut für Experimentelle Kernphysik, Karlsruhe, Germany

C. Barth, C. Baus, J. Berger, E. Butz, T. Chwalek, F. Colombo, W. De Boer, A. Dierlamm, S. Fink, R. Friese, M. Giffels, A. Gilbert, D. Haitz, F. Hartmann¹³, S.M. Heindl, U. Husemann, I. Katkov¹⁴, P. Lobelle Pardo, B. Maier, H. Mildner, M.U. Mozer, T. Müller, Th. Müller, M. Plagge, G. Quast, K. Rabbertz, S. Röcker, F. Roscher, M. Schröder, I. Shvetsov, G. Sieber, H.J. Simonis, R. Ulrich, J. Wagner-Kuhr, S. Wayand, M. Weber, T. Weiler, S. Williamson, C. Wöhrmann, R. Wolf

Institute of Nuclear and Particle Physics (INPP), NCSR Demokritos, Aghia Paraskevi, Greece

G. Anagnostou, G. Daskalakis, T. Gerasis, V.A. Giakoumopoulou, A. Kyriakis, D. Loukas, I. Topsis-Giotis

National and Kapodistrian University of Athens, Athens, Greece

A. Agapitos, S. Kesisoglou, A. Panagiotou, N. Saoulidou, E. Tziaferi

University of Ioánnina, Ioánnina, Greece

I. Evangelou, G. Flouris, C. Foudas, P. Kokkas, N. Loukas, N. Manthos, I. Papadopoulos, E. Paradis

MTA-ELTE Lendület CMS Particle and Nuclear Physics Group, Eötvös Loránd University, Budapest, Hungary

N. Filipovic

Wigner Research Centre for Physics, Budapest, Hungary

G. Bencze, C. Hajdu, P. Hidas, D. Horvath¹⁹, F. Sikler, V. Veszpremi, G. Vesztergombi²⁰, A.J. Zsigmond

Institute of Nuclear Research ATOMKI, Debrecen, Hungary

N. Beni, S. Czellar, J. Karancsi²¹, A. Makovec, J. Molnar, Z. Szillasi

University of Debrecen, Debrecen, Hungary

M. Bartók²⁰, P. Raics, Z.L. Trocsanyi, B. Ujvari

National Institute of Science Education and Research, Bhubaneswar, India

S. Bahinipati, S. Choudhury²², P. Mal, K. Mandal, A. Nayak²³, D.K. Sahoo, N. Sahoo, S.K. Swain

Panjab University, Chandigarh, India

S. Bansal, S.B. Beri, V. Bhatnagar, R. Chawla, U.Bhawandeep, A.K. Kalsi, A. Kaur, M. Kaur, R. Kumar, A. Mehta, M. Mittal, J.B. Singh, G. Walia

University of Delhi, Delhi, India

Ashok Kumar, A. Bhardwaj, B.C. Choudhary, R.B. Garg, S. Keshri, A. Kumar, S. Malhotra, M. Naimuddin, N. Nishu, K. Ranjan, R. Sharma, V. Sharma

Saha Institute of Nuclear Physics, Kolkata, India

R. Bhattacharya, S. Bhattacharya, K. Chatterjee, S. Dey, S. Dutt, S. Dutta, S. Ghosh, N. Majumdar, A. Modak, K. Mondal, S. Mukhopadhyay, S. Nandan, A. Purohit, A. Roy, D. Roy, S. Roy Chowdhury, S. Sarkar, M. Sharan, S. Thakur

Indian Institute of Technology Madras, Madras, India

P.K. Behera

Bhabha Atomic Research Centre, Mumbai, India

R. Chudasama, D. Dutta, V. Jha, V. Kumar, A.K. Mohanty¹³, P.K. Netrakanti, L.M. Pant, P. Shukla, A. Topkar

Tata Institute of Fundamental Research-A, Mumbai, India

T. Aziz, S. Dugad, G. Kole, B. Mahakud, S. Mitra, G.B. Mohanty, N. Sur, B. Sutar

Tata Institute of Fundamental Research-B, Mumbai, India

S. Banerjee, S. Bhowmik²⁴, R.K. Dewanjee, S. Ganguly, M. Guchait, Sa. Jain, S. Kumar, M. Maity²⁴, G. Majumder, K. Mazumdar, B. Parida, T. Sarkar²⁴, N. Wickramage²⁵

Indian Institute of Science Education and Research (IISER), Pune, India

S. Chauhan, S. Dube, V. Hegde, A. Kapoor, K. Kothekar, A. Rane, S. Sharma

Institute for Research in Fundamental Sciences (IPM), Tehran, Iran

H. Behnamian, S. Chenarani²⁶, E. Eskandari Tadavani, S.M. Etesami²⁶, A. Fahim²⁷, M. Khakzad, M. Mohammadi Najafabadi, M. Naseri, S. Paktinat Mehdiabadi, F. Rezaei Hosseinabadi, B. Safarzadeh²⁸, M. Zeinali

University College Dublin, Dublin, Ireland

M. Felcini, M. Grunewald

INFN Sezione di Bari ^a, Università di Bari ^b, Politecnico di Bari ^c, Bari, Italy

M. Abbrescia^{a,b}, C. Calabria^{a,b}, C. Caputo^{a,b}, A. Colaleo^a, D. Creanza^{a,c}, L. Cristella^{a,b}, N. De Filippis^{a,c}, M. De Palma^{a,b}, L. Fiore^a, G. Iaselli^{a,c}, G. Maggi^{a,c}, M. Maggi^a, G. Miniello^{a,b}, S. My^{a,b}, S. Nuzzo^{a,b}, A. Pompili^{a,b}, G. Pugliese^{a,c}, R. Radogna^{a,b}, A. Ranieri^a, G. Selvaggi^{a,b}, L. Silvestris^{a,13}, R. Venditti^{a,b}, P. Verwilligen^a

INFN Sezione di Bologna ^a, Università di Bologna ^b, Bologna, Italy

G. Abbiendi^a, C. Battilana, D. Bonacorsi^{a,b}, S. Braibant-Giacomelli^{a,b}, L. Brigliadori^{a,b}, R. Campanini^{a,b}, P. Capiluppi^{a,b}, A. Castro^{a,b}, F.R. Cavallo^a, S.S. Chhibra^{a,b}, G. Codispoti^{a,b}, M. Cuffiani^{a,b}, G.M. Dallavalle^a, F. Fabbri^a, A. Fanfani^{a,b}, D. Fasanella^{a,b}, P. Giacomelli^a, C. Grandi^a, L. Guiducci^{a,b}, S. Marcellini^a, G. Masetti^a, A. Montanari^a, F.L. Navarria^{a,b}, A. Perrotta^a, A.M. Rossi^{a,b}, T. Rovelli^{a,b}, G.P. Siroli^{a,b}, N. Tosi^{a,b,13}

INFN Sezione di Catania ^a, Università di Catania ^b, Catania, Italy

S. Albergo^{a,b}, M. Chiorboli^{a,b}, S. Costa^{a,b}, A. Di Mattia^a, F. Giordano^{a,b}, R. Potenza^{a,b}, A. Tricomi^{a,b}, C. Tuve^{a,b}

INFN Sezione di Firenze ^a, Università di Firenze ^b, Firenze, Italy

G. Barbagli^a, V. Ciulli^{a,b}, C. Civinini^a, R. D'Alessandro^{a,b}, E. Focardi^{a,b}, V. Gori^{a,b}, P. Lenzi^{a,b}, M. Meschini^a, S. Paoletti^a, G. Sguazzoni^a, L. Viliani^{a,b,13}

INFN Laboratori Nazionali di Frascati, Frascati, Italy

L. Benussi, S. Bianco, F. Fabbri, D. Piccolo, F. Primavera¹³

INFN Sezione di Genova ^a, Università di Genova ^b, Genova, Italy

V. Calvelli^{a,b}, F. Ferro^a, M. Lo Vetere^{a,b}, M.R. Monge^{a,b}, E. Robutti^a, S. Tosi^{a,b}

INFN Sezione di Milano-Bicocca ^a, Università di Milano-Bicocca ^b, Milano, Italy

L. Brianza, M.E. Dinardo^{a,b}, S. Fiorendi^{a,b}, S. Gennai^a, A. Ghezzi^{a,b}, P. Govoni^{a,b}, S. Malvezzi^a, R.A. Manzoni^{a,b,13}, B. Marzocchi^{a,b}, D. Menasce^a, L. Moroni^a, M. Paganoni^{a,b}, D. Pedrini^a, S. Pigazzini, S. Ragazzi^{a,b}, T. Tabarelli de Fatis^{a,b}

INFN Sezione di Napoli ^a, Università di Napoli 'Federico II' ^b, Napoli, Italy, Università della Basilicata ^c, Potenza, Italy, Università G. Marconi ^d, Roma, Italy

S. Buontempo^a, N. Cavallo^{a,c}, G. De Nardo, S. Di Guida^{a,d,13}, M. Esposito^{a,b}, F. Fabozzi^{a,c}, A.O.M. Iorio^{a,b}, G. Lanza^a, L. Lista^a, S. Meola^{a,d,13}, P. Paolucci^{a,13}, C. Sciacca^{a,b}, F. Thyssen

INFN Sezione di Padova ^a, Università di Padova ^b, Padova, Italy, Università di Trento ^c, Trento, Italy

P. Azzi^{a,13}, N. Bacchetta^a, L. Benato^{a,b}, D. Bisello^{a,b}, A. Boletti^{a,b}, R. Carlin^{a,b}, A. Carvalho Antunes De Oliveira^{a,b}, P. Checchia^a, M. Dall'Osso^{a,b}, P. De Castro Manzano^a, T. Dorigo^a, U. Dosselli^a, F. Gasparini^{a,b}, U. Gasparini^{a,b}, A. Gozzelino^a, S. Lacaprara^a, M. Margoni^{a,b}, A.T. Meneguzzo^{a,b}, J. Pazzini^{a,b,13}, N. Pozzobon^{a,b}, P. Ronchese^{a,b}, F. Simonetto^{a,b}, E. Torassa^a, M. Zanetti, P. Zotto^{a,b}, A. Zucchetta^{a,b}, G. Zumerle^{a,b}

INFN Sezione di Pavia ^a, Università di Pavia ^b, Pavia, Italy

A. Braghieri^a, A. Magnani^{a,b}, P. Montagna^{a,b}, S.P. Ratti^{a,b}, V. Re^a, C. Riccardi^{a,b}, P. Salvini^a, I. Vai^{a,b}, P. Vitulo^{a,b}

INFN Sezione di Perugia ^a, Università di Perugia ^b, Perugia, Italy

L. Alunni Solestizi^{a,b}, G.M. Bilei^a, D. Ciangottini^{a,b}, L. Fanò^{a,b}, P. Lariccia^{a,b}, R. Leonardi^{a,b}, G. Mantovani^{a,b}, M. Menichelli^a, A. Saha^a, A. Santocchia^{a,b}

INFN Sezione di Pisa ^a, Università di Pisa ^b, Scuola Normale Superiore di Pisa ^c, Pisa, Italy

K. Androsov^{a,29}, P. Azzurri^{a,13}, G. Bagliesi^a, J. Bernardini^a, T. Boccali^a, R. Castaldi^a, M.A. Ciocci^{a,29}, R. Dell'Orso^a, S. Donato^{a,c}, G. Fedi, A. Giassi^a, M.T. Grippo^{a,29}, F. Ligabue^{a,c}, T. Lomtadze^a, L. Martini^{a,b}, A. Messineo^{a,b}, F. Palla^a, A. Rizzi^{a,b}, A. Savoy-Navarro^{a,30}, P. Spagnolo^a, R. Tenchini^a, G. Tonelli^{a,b}, A. Venturi^a, P.G. Verdini^a

INFN Sezione di Roma ^a, Università di Roma ^b, Roma, Italy

L. Barone^{a,b}, F. Cavallari^a, M. Cipriani^{a,b}, G. D'imperio^{a,b,13}, D. Del Re^{a,b,13}, M. Diemoz^a, S. Gelli^{a,b}, C. Jorda^a, E. Longo^{a,b}, F. Margaroli^{a,b}, P. Meridiani^a, G. Organtini^{a,b}, R. Paramatti^a, F. Preiato^{a,b}, S. Rahatlou^{a,b}, C. Rovelli^a, F. Santanastasio^{a,b}

INFN Sezione di Torino ^a, Università di Torino ^b, Torino, Italy, Università del Piemonte Orientale ^c, Novara, Italy

N. Amapane^{a,b}, R. Arcidiacono^{a,c,13}, S. Argiro^{a,b}, M. Arneodo^{a,c}, N. Bartosik^a, R. Bellan^{a,b}, C. Biino^a, N. Cartiglia^a, F. Cenna^{a,b}, M. Costa^{a,b}, R. Covarelli^{a,b}, A. Degano^{a,b}, N. Demaria^a, L. Finco^{a,b}, B. Kiani^{a,b}, C. Mariotti^a, S. Maselli^a, E. Migliore^{a,b}, V. Monaco^{a,b}, E. Monteil^{a,b}, M.M. Obertino^{a,b}, L. Pacher^{a,b}, N. Pastrone^a, M. Pelliccioni^a, G.L. Pinna Angioni^{a,b}, F. Ravera^{a,b},

A. Romero^{a,b}, M. Ruspa^{a,c}, R. Sacchi^{a,b}, K. Shchelina^{a,b}, V. Sola^a, A. Solano^{a,b}, A. Staiano^a, P. Traczyk^{a,b}

INFN Sezione di Trieste ^a, Università di Trieste ^b, Trieste, Italy

S. Belforte^a, M. Casarsa^a, F. Cossutti^a, G. Della Ricca^{a,b}, C. La Licata^{a,b}, A. Schizzi^{a,b}, A. Zanetti^a

Kyungpook National University, Daegu, Korea

D.H. Kim, G.N. Kim, M.S. Kim, S. Lee, S.W. Lee, Y.D. Oh, S. Sekmen, D.C. Son, Y.C. Yang

Chonbuk National University, Jeonju, Korea

A. Lee

Hanyang University, Seoul, Korea

J.A. Brochero Cifuentes, T.J. Kim

Korea University, Seoul, Korea

S. Cho, S. Choi, Y. Go, D. Gyun, S. Ha, B. Hong, Y. Jo, Y. Kim, B. Lee, K. Lee, K.S. Lee, S. Lee, J. Lim, S.K. Park, Y. Roh

Seoul National University, Seoul, Korea

J. Almond, J. Kim, S.B. Oh, S.h. Seo, U.K. Yang, H.D. Yoo, G.B. Yu

University of Seoul, Seoul, Korea

M. Choi, H. Kim, H. Kim, J.H. Kim, J.S.H. Lee, I.C. Park, G. Ryu, M.S. Ryu

Sungkyunkwan University, Suwon, Korea

Y. Choi, J. Goh, C. Hwang, J. Lee, I. Yu

Vilnius University, Vilnius, Lithuania

V. Dudenas, A. Juodagalvis, J. Vaitkus

National Centre for Particle Physics, Universiti Malaya, Kuala Lumpur, Malaysia

I. Ahmed, Z.A. Ibrahim, J.R. Komaragiri, M.A.B. Md Ali³¹, F. Mohamad Idris³², W.A.T. Wan Abdullah, M.N. Yusli, Z. Zolkapli

Centro de Investigacion y de Estudios Avanzados del IPN, Mexico City, Mexico

E. Casimiro Linares, H. Castilla-Valdez, E. De La Cruz-Burelo, I. Heredia-De La Cruz³³, A. Hernandez-Almada, R. Lopez-Fernandez, R. Magaña Villalba, J. Mejia Guisao, A. Sanchez-Hernandez

Universidad Iberoamericana, Mexico City, Mexico

S. Carrillo Moreno, C. Oropeza Barrera, F. Vazquez Valencia

Benemerita Universidad Autonoma de Puebla, Puebla, Mexico

S. Carpinteyro, I. Pedraza, H.A. Salazar Ibarquen, C. Uribe Estrada

Universidad Autónoma de San Luis Potosí, San Luis Potosí, Mexico

A. Morelos Pineda

University of Auckland, Auckland, New Zealand

D. Krofcheck

University of Canterbury, Christchurch, New Zealand

P.H. Butler

National Centre for Physics, Quaid-I-Azam University, Islamabad, Pakistan

A. Ahmad, M. Ahmad, Q. Hassan, H.R. Hoorani, W.A. Khan, M.A. Shah, M. Shoaib, M. Waqas

National Centre for Nuclear Research, Swierk, Poland

H. Bialkowska, M. Bluj, B. Boimska, T. Frueboes, M. Górski, M. Kazana, K. Nawrocki, K. Romanowska-Rybinska, M. Szleper, P. Zalewski

Institute of Experimental Physics, Faculty of Physics, University of Warsaw, Warsaw, Poland

K. Bunkowski, A. Byszuk³⁴, K. Doroba, A. Kalinowski, M. Konecki, J. Krolikowski, M. Misiura, M. Olszewski, M. Walczak

Laboratório de Instrumentação e Física Experimental de Partículas, Lisboa, Portugal

P. Bargassa, C. Beirão Da Cruz E Silva, A. Di Francesco, P. Faccioli, P.G. Ferreira Parracho, M. Gallinaro, J. Hollar, N. Leonardo, L. Lloret Iglesias, M.V. Nemallapudi, J. Rodrigues Antunes, J. Seixas, O. Toldaiev, D. Vadrucio, J. Varela, P. Vischia

Joint Institute for Nuclear Research, Dubna, Russia

I. Belotelov, P. Bunin, M. Gavrilenko, I. Golutvin, I. Gorbunov, A. Kamenev, V. Karjavin, A. Lanev, A. Malakhov, V. Matveev^{35,36}, P. Moiseenz, V. Palichik, V. Perelygin, M. Savina, S. Shmatov, N. Skatchkov, V. Smirnov, N. Voytishin, A. Zarubin

Petersburg Nuclear Physics Institute, Gatchina (St. Petersburg), Russia

L. Chtchypounov, V. Golovtsov, Y. Ivanov, V. Kim³⁷, E. Kuznetsova³⁸, V. Murzin, V. Oreshkin, V. Sulimov, A. Vorobyev

Institute for Nuclear Research, Moscow, Russia

Yu. Andreev, A. Dermenev, S. Gninenko, N. Golubev, A. Karneyeu, M. Kirsanov, N. Krasnikov, A. Pashenkov, D. Tlisov, A. Toropin

Institute for Theoretical and Experimental Physics, Moscow, Russia

V. Epshteyn, V. Gavrillov, N. Lychkovskaya, V. Popov, I. Pozdnyakov, G. Safronov, A. Spiridonov, M. Toms, E. Vlasov, A. Zhokin

Moscow Institute of Physics and Technology

A. Bylinkin³⁶

National Research Nuclear University 'Moscow Engineering Physics Institute' (MEPhI), Moscow, Russia

R. Chistov³⁹, V. Rusinov, E. Tarkovskii

P.N. Lebedev Physical Institute, Moscow, Russia

V. Andreev, M. Azarkin³⁶, I. Dremin³⁶, M. Kirakosyan, A. Leonidov³⁶, S.V. Rusakov, A. Terkulov

Skobeltsyn Institute of Nuclear Physics, Lomonosov Moscow State University, Moscow, Russia

A. Baskakov, A. Belyaev, E. Boos, M. Dubinin⁴⁰, L. Dudko, A. Ershov, A. Gribushin, V. Klyukhin, O. Kodolova, I. Lokhtin, I. Miagkov, S. Obraztsov, S. Petrushanko, V. Savrin, A. Snigirev

State Research Center of Russian Federation, Institute for High Energy Physics, Protvino, Russia

I. Azhgirey, I. Bayshev, S. Bitioukov, D. Elumakhov, V. Kachanov, A. Kalinin, D. Konstantinov, V. Krychkin, V. Petrov, R. Ryutin, A. Sobol, S. Troshin, N. Tyurin, A. Uzunian, A. Volkov

University of Belgrade, Faculty of Physics and Vinca Institute of Nuclear Sciences, Belgrade, Serbia

P. Adzic⁴¹, P. Cirkovic, D. Devetak, M. Dordevic, J. Milosevic, V. Rekovic

Centro de Investigaciones Energéticas Medioambientales y Tecnológicas (CIEMAT), Madrid, Spain

J. Alcaraz Maestre, M. Barrio Luna, E. Calvo, M. Cerrada, M. Chamizo Llatas, N. Colino, B. De La Cruz, A. Delgado Peris, A. Escalante Del Valle, C. Fernandez Bedoya, J.P. Fernández Ramos, J. Flix, M.C. Fouz, P. Garcia-Abia, O. Gonzalez Lopez, S. Goy Lopez, J.M. Hernandez, M.I. Josa, E. Navarro De Martino, A. Pérez-Calero Yzquierdo, J. Puerta Pelayo, A. Quintario Olmeda, I. Redondo, L. Romero, M.S. Soares

Universidad Autónoma de Madrid, Madrid, Spain

J.F. de Trocóniz, M. Missiroli, D. Moran

Universidad de Oviedo, Oviedo, Spain

J. Cuevas, J. Fernandez Menendez, I. Gonzalez Caballero, J.R. González Fernández, E. Palencia Cortezon, S. Sanchez Cruz, I. Suárez Andrés, J.M. Vizán Garcia

Instituto de Física de Cantabria (IFCA), CSIC-Universidad de Cantabria, Santander, Spain

I.J. Cabrillo, A. Calderon, J.R. Castiñeiras De Saa, E. Curras, M. Fernandez, J. Garcia-Ferrero, G. Gomez, A. Lopez Virto, J. Marco, C. Martinez Rivero, F. Matorras, J. Piedra Gomez, T. Rodrigo, A. Ruiz-Jimeno, L. Scodellaro, N. Trevisani, I. Vila, R. Vilar Cortabitarte

CERN, European Organization for Nuclear Research, Geneva, Switzerland

D. Abbaneo, E. Auffray, G. Auzinger, M. Bachtis, P. Baillon, A.H. Ball, D. Barney, P. Bloch, A. Bocci, A. Bonato, C. Botta, T. Camporesi, R. Castello, M. Cepeda, G. Cerminara, M. D'Alfonso, D. d'Enterria, A. Dabrowski, V. Daponte, A. David, M. De Gruttola, F. De Guio, A. De Roeck, E. Di Marco⁴², M. Dobson, B. Dorney, T. du Pree, D. Duggan, M. Dünser, N. Dupont, A. Elliott-Peisert, S. Fartoukh, G. Franzoni, J. Fulcher, W. Funk, D. Gigi, K. Gill, M. Girone, F. Glege, D. Gulhan, S. Gundacker, M. Guthoff, J. Hammer, P. Harris, J. Hegeman, V. Innocente, P. Janot, H. Kirschenmann, V. Knünz, A. Kornmayer¹³, M.J. Kortelainen, K. Kousouris, M. Krammer¹, P. Lecoq, C. Lourenço, M.T. Lucchini, L. Malgeri, M. Mannelli, A. Martelli, F. Meijers, S. Mersi, E. Meschi, F. Moortgat, S. Morovic, M. Mulders, H. Neugebauer, S. Orfanelli, L. Orsini, L. Pape, E. Perez, M. Peruzzi, A. Petrilli, G. Petrucciani, A. Pfeiffer, M. Pierini, A. Racz, T. Reis, G. Rolandi⁴³, M. Rovere, M. Ruan, H. Sakulin, J.B. Sauvan, C. Schäfer, C. Schwick, M. Seidel, A. Sharma, P. Silva, M. Simon, P. Sphicas⁴⁴, J. Steggemann, M. Stoye, Y. Takahashi, M. Tosi, D. Treille, A. Triossi, A. Tsirou, V. Veckalns⁴⁵, G.I. Veres²⁰, N. Wardle, H.K. Wöhri, A. Zagozdinska³⁴, W.D. Zeuner

Paul Scherrer Institut, Villigen, Switzerland

W. Bertl, K. Deiters, W. Erdmann, R. Horisberger, Q. Ingram, H.C. Kaestli, D. Kotlinski, U. Langenegger, T. Rohe

Institute for Particle Physics, ETH Zurich, Zurich, Switzerland

F. Bachmair, L. Bäni, L. Bianchini, B. Casal, G. Dissertori, M. Dittmar, M. Donegà, P. Eller, C. Grab, C. Heidegger, D. Hits, J. Hoss, G. Kasieczka, P. Lecomte[†], W. Lustermann, B. Mangano, M. Marionneau, P. Martinez Ruiz del Arbol, M. Masciovecchio, M.T. Meinhard, D. Meister, F. Micheli, P. Musella, F. Nessi-Tedaldi, F. Pandolfi, J. Pata, F. Pauss, G. Perrin, L. Perrozzi, M. Quittnat, M. Rossini, M. Schönenberger, A. Starodumov⁴⁶, V.R. Tavolaro, K. Theofilatos, R. Wallny

Universität Zürich, Zurich, Switzerland

T.K. Aarrestad, C. Amsler⁴⁷, L. Caminada, M.F. Canelli, V. Chiochia, A. De Cosa, C. Galloni, A. Hinzmann, T. Hreus, B. Kilminster, C. Lange, J. Ngadiuba, D. Pinna, G. Rauco, P. Robmann, D. Salerno, Y. Yang

National Central University, Chung-Li, Taiwan

V. Candelise, T.H. Doan, Sh. Jain, R. Khurana, M. Konyushikhin, C.M. Kuo, W. Lin, Y.J. Lu, A. Pozdnyakov, S.S. Yu

National Taiwan University (NTU), Taipei, Taiwan

Arun Kumar, P. Chang, Y.H. Chang, Y.W. Chang, Y. Chao, K.F. Chen, P.H. Chen, C. Dietz, F. Fiori, W.-S. Hou, Y. Hsiung, Y.F. Liu, R.-S. Lu, M. Miñano Moya, E. Paganis, A. Psallidas, J.f. Tsai, Y.M. Tzeng

Chulalongkorn University, Faculty of Science, Department of Physics, Bangkok, Thailand

B. Asavapibhop, G. Singh, N. Srimanobhas, N. Suwonjandee

Cukurova University, Adana, Turkey

A. Adiguzel, S. Cerci⁴⁸, S. Damarseckin, Z.S. Demiroglu, C. Dozen, I. Dumanoglu, S. Girgis, G. Gokbulut, Y. Guler, E. Gurpinar, I. Hos, E.E. Kangal⁴⁹, O. Kara, A. Kayis Topaksu, U. Kiminsu, M. Oglakci, G. Onengut⁵⁰, K. Ozdemir⁵¹, D. Sunar Cerci⁴⁸, H. Topakli⁵², S. Turkcapar, I.S. Zorbakir, C. Zorbilmez

Middle East Technical University, Physics Department, Ankara, Turkey

B. Bilin, S. Bilmis, B. Isildak⁵³, G. Karapinar⁵⁴, M. Yalvac, M. Zeyrek

Bogazici University, Istanbul, Turkey

E. Gülmez, M. Kaya⁵⁵, O. Kaya⁵⁶, E.A. Yetkin⁵⁷, T. Yetkin⁵⁸

Istanbul Technical University, Istanbul, Turkey

A. Cakir, K. Cankocak, S. Sen⁵⁹

Institute for Scintillation Materials of National Academy of Science of Ukraine, Kharkov, Ukraine

B. Grynyov

National Scientific Center, Kharkov Institute of Physics and Technology, Kharkov, Ukraine

L. Levchuk, P. Sorokin

University of Bristol, Bristol, United Kingdom

R. Aggleton, F. Ball, L. Beck, J.J. Brooke, D. Burns, E. Clement, D. Cussans, H. Flacher, J. Goldstein, M. Grimes, G.P. Heath, H.F. Heath, J. Jacob, L. Kreczko, C. Lucas, D.M. Newbold⁶⁰, S. Paramesvaran, A. Poll, T. Sakuma, S. Seif El Nasr-storey, D. Smith, V.J. Smith

Rutherford Appleton Laboratory, Didcot, United Kingdom

K.W. Bell, A. Belyaev⁶¹, C. Brew, R.M. Brown, L. Calligaris, D. Cieri, D.J.A. Cockerill, J.A. Coughlan, K. Harder, S. Harper, E. Olaiya, D. Petyt, C.H. Shepherd-Themistocleous, A. Thea, I.R. Tomalin, T. Williams

Imperial College, London, United Kingdom

M. Baber, R. Bainbridge, O. Buchmuller, A. Bundock, D. Burton, S. Casasso, M. Citron, D. Colling, L. Corpe, P. Dauncey, G. Davies, A. De Wit, M. Della Negra, P. Dunne, A. Elwood, D. Futyan, Y. Haddad, G. Hall, G. Iles, T. James, R. Lane, C. Laner, R. Lucas⁶⁰, L. Lyons, A.-M. Magnan, S. Malik, L. Mastrolorenzo, J. Nash, A. Nikitenko⁴⁶, J. Pela, B. Penning, M. Pesaresi, D.M. Raymond, A. Richards, A. Rose, C. Seez, S. Summers, A. Tapper, K. Uchida, M. Vazquez Acosta⁶², T. Virdee¹³, J. Wright, S.C. Zenz

Brunel University, Uxbridge, United Kingdom

J.E. Cole, P.R. Hobson, A. Khan, P. Kyberd, D. Leslie, I.D. Reid, P. Symonds, L. Teodorescu, M. Turner

Baylor University, Waco, USA

A. Borzou, K. Call, J. Dittmann, K. Hatakeyama, H. Liu, N. Pastika

The University of Alabama, Tuscaloosa, USA

O. Charaf, S.I. Cooper, C. Henderson, P. Rumerio

Boston University, Boston, USA

D. Arcaro, A. Avetisyan, T. Bose, D. Gastler, D. Rankin, C. Richardson, J. Rohlf, L. Sulak, D. Zou

Brown University, Providence, USA

G. Benelli, E. Berry, D. Cutts, A. Garabedian, J. Hakala, U. Heintz, J.M. Hogan, O. Jesus, E. Laird, G. Landsberg, Z. Mao, M. Narain, S. Piperov, S. Sagir, E. Spencer, R. Syarif

University of California, Davis, Davis, USA

R. Breedon, G. Breto, D. Burns, M. Calderon De La Barca Sanchez, S. Chauhan, M. Chertok, J. Conway, R. Conway, P.T. Cox, R. Erbacher, C. Flores, G. Funk, M. Gardner, W. Ko, R. Lander, C. Mclean, M. Mulhearn, D. Pellett, J. Pilot, F. Ricci-Tam, S. Shalhout, J. Smith, M. Squires, D. Stolp, M. Tripathi, S. Wilbur, R. Yohay

University of California, Los Angeles, USA

R. Cousins, P. Everaerts, A. Florent, J. Hauser, M. Ignatenko, D. Saltzberg, E. Takasugi, V. Valuev, M. Weber

University of California, Riverside, Riverside, USA

K. Burt, R. Clare, J. Ellison, J.W. Gary, G. Hanson, J. Heilman, P. Jandir, E. Kennedy, F. Lacroix, O.R. Long, M. Malberti, M. Olmedo Negrete, M.I. Paneva, A. Shrinivas, H. Wei, S. Wimpenny, B. R. Yates

University of California, San Diego, La Jolla, USA

J.G. Branson, G.B. Cerati, S. Cittolin, M. Derdzinski, R. Gerosa, A. Holzner, D. Klein, V. Krutelyov, J. Letts, I. Macneill, D. Olivito, S. Padhi, M. Pieri, M. Sani, V. Sharma, S. Simon, M. Tadel, A. Vartak, S. Wasserbaech⁶³, C. Welke, J. Wood, F. Würthwein, A. Yagil, G. Zevi Della Porta

University of California, Santa Barbara - Department of Physics, Santa Barbara, USA

R. Bhandari, J. Bradmiller-Feld, C. Campagnari, A. Dishaw, V. Dutta, K. Flowers, M. Franco Sevilla, P. Geffert, C. George, F. Golf, L. Gouskos, J. Gran, R. Heller, J. Incandela, N. Mccoll, S.D. Mullin, A. Ovcharova, J. Richman, D. Stuart, I. Suarez, C. West, J. Yoo

California Institute of Technology, Pasadena, USA

D. Anderson, A. Apresyan, J. Bendavid, A. Bornheim, J. Bunn, Y. Chen, J. Duarte, J.M. Lawhorn, A. Mott, H.B. Newman, C. Pena, M. Spiropulu, J.R. Vlimant, S. Xie, R.Y. Zhu

Carnegie Mellon University, Pittsburgh, USA

M.B. Andrews, V. Azzolini, B. Carlson, T. Ferguson, M. Paulini, J. Russ, M. Sun, H. Vogel, I. Vorobiev

University of Colorado Boulder, Boulder, USA

J.P. Cumalat, W.T. Ford, F. Jensen, A. Johnson, M. Krohn, T. Mulholland, K. Stenson, S.R. Wagner

Cornell University, Ithaca, USA

J. Alexander, J. Chaves, J. Chu, S. Dittmer, K. Mcdermott, N. Mirman, G. Nicolas Kaufman, J.R. Patterson, A. Rinkevicius, A. Ryd, L. Skinnari, L. Soffi, S.M. Tan, Z. Tao, J. Thom, J. Tucker, P. Wittich, M. Zientek

Fairfield University, Fairfield, USA

D. Winn

Fermi National Accelerator Laboratory, Batavia, USA

S. Abdullin, M. Albrow, G. Apollinari, S. Banerjee, L.A.T. Bauerdick, A. Beretvas, J. Berryhill, P.C. Bhat, G. Bolla, K. Burkett, J.N. Butler, H.W.K. Cheung, F. Chlebana, S. Cihangir, M. Cremonesi, V.D. Elvira, I. Fisk, J. Freeman, E. Gottschalk, L. Gray, D. Green, S. Grünendahl, O. Gutsche, D. Hare, R.M. Harris, S. Hasegawa, J. Hirschauer, Z. Hu, B. Jayatilaka, S. Jindariani, M. Johnson, U. Joshi, B. Klima, B. Kreis, S. Lammel, J. Linacre, D. Lincoln, R. Lipton, T. Liu, R. Lopes De Sá, J. Lykken, K. Maeshima, N. Magini, J.M. Marraffino, S. Maruyama, D. Mason, P. McBride, P. Merkel, S. Mrenna, S. Nahn, C. Newman-Holmes[†], V. O'Dell, K. Pedro, O. Prokofyev, G. Rakness, L. Ristori, E. Sexton-Kennedy, A. Soha, W.J. Spalding, L. Spiegel, S. Stoynev, N. Strobbe, L. Taylor, S. Tkaczyk, N.V. Tran, L. Uplegger, E.W. Vaandering, C. Vernieri, M. Verzocchi, R. Vidal, M. Wang, H.A. Weber, A. Whitbeck

University of Florida, Gainesville, USA

D. Acosta, P. Avery, P. Bortignon, D. Bourilkov, A. Brinkerhoff, A. Carnes, M. Carver, D. Curry, S. Das, R.D. Field, I.K. Furic, J. Konigsberg, A. Korytov, P. Ma, K. Matchev, H. Mei, P. Milenovic⁶⁴, G. Mitselmakher, D. Rank, L. Shchutska, D. Sperka, L. Thomas, J. Wang, S. Wang, J. Yelton

Florida International University, Miami, USA

S. Linn, P. Markowitz, G. Martinez, J.L. Rodriguez

Florida State University, Tallahassee, USA

A. Ackert, J.R. Adams, T. Adams, A. Askew, S. Bein, B. Diamond, S. Hagopian, V. Hagopian, K.F. Johnson, A. Khatiwada, H. Prosper, A. Santra, M. Weinberg

Florida Institute of Technology, Melbourne, USA

M.M. Baarmand, V. Bhopatkar, S. Colafranceschi⁶⁵, M. Hohlmann, D. Noonan, T. Roy, F. Yumiceva

University of Illinois at Chicago (UIC), Chicago, USA

M.R. Adams, L. Apanasevich, D. Berry, R.R. Betts, I. Bucinskaite, R. Cavanaugh, O. Evdokimov, L. Gauthier, C.E. Gerber, D.J. Hofman, P. Kurt, C. O'Brien, I.D. Sandoval Gonzalez, P. Turner, N. Varelas, H. Wang, Z. Wu, M. Zakaria, J. Zhang

The University of Iowa, Iowa City, USA

B. Bilki⁶⁶, W. Clarida, K. Dilsiz, S. Durgut, R.P. Gandrajula, M. Haytmyradov, V. Khristenko, J.-P. Merlo, H. Mermerkaya⁶⁷, A. Mestvirishvili, A. Moeller, J. Nachtman, H. Ogul, Y. Onel, F. Ozok⁶⁸, A. Penzo, C. Snyder, E. Tiras, J. Wetzel, K. Yi

Johns Hopkins University, Baltimore, USA

I. Anderson, B. Blumenfeld, A. Cocoros, N. Eminizer, D. Fehling, L. Feng, A.V. Gritsan, P. Maksimovic, M. Osherson, J. Roskes, U. Sarica, M. Swartz, M. Xiao, Y. Xin, C. You

The University of Kansas, Lawrence, USA

A. Al-bataineh, P. Baringer, A. Bean, J. Bowen, C. Bruner, J. Castle, R.P. Kenny III, A. Kropivnitskaya, D. Majumder, W. Mcbrayer, M. Murray, S. Sanders, R. Stringer, J.D. Tapia Takaki, Q. Wang

Kansas State University, Manhattan, USA

A. Ivanov, K. Kaadze, S. Khalil, M. Makouski, Y. Maravin, A. Mohammadi, L.K. Saini, N. Skhirtladze, S. Toda

Lawrence Livermore National Laboratory, Livermore, USA

D. Lange, F. Rebassoo, D. Wright

University of Maryland, College Park, USA

C. Anelli, A. Baden, O. Baron, A. Belloni, B. Calvert, S.C. Eno, C. Ferraioli, J.A. Gomez, N.J. Hadley, S. Jabeen, R.G. Kellogg, T. Kolberg, J. Kunkle, Y. Lu, A.C. Mignerey, Y.H. Shin, A. Skuja, M.B. Tonjes, S.C. Tonwar

Massachusetts Institute of Technology, Cambridge, USA

D. Abercrombie, B. Allen, A. Apyan, R. Barbieri, A. Baty, R. Bi, K. Bierwagen, S. Brandt, W. Busza, I.A. Cali, Z. Demiragli, L. Di Matteo, G. Gomez Ceballos, M. Goncharov, D. Hsu, Y. Iiyama, G.M. Innocenti, M. Klute, D. Kovalskyi, K. Krajczar, Y.S. Lai, Y.-J. Lee, A. Levin, P.D. Luckey, A.C. Marini, C. Mcginn, C. Mironov, S. Narayanan, X. Niu, C. Paus, C. Roland, G. Roland, J. Salfeld-Nebgen, G.S.F. Stephans, K. Sumorok, K. Tatar, M. Varma, D. Velicanu, J. Veverka, J. Wang, T.W. Wang, B. Wyslouch, M. Yang, V. Zhukova

University of Minnesota, Minneapolis, USA

A.C. Benvenuti, R.M. Chatterjee, A. Evans, A. Finkel, A. Gude, P. Hansen, S. Kalafut, S.C. Kao, Y. Kubota, Z. Lesko, J. Mans, S. Nourbakhsh, N. Ruckstuhl, R. Rusack, N. Tambe, J. Turkewitz

University of Mississippi, Oxford, USA

J.G. Acosta, S. Oliveros

University of Nebraska-Lincoln, Lincoln, USA

E. Avdeeva, R. Bartek, K. Bloom, S. Bose, D.R. Claes, A. Dominguez, C. Fangmeier, R. Gonzalez Suarez, R. Kamalieddin, D. Knowlton, I. Kravchenko, A. Malta Rodrigues, F. Meier, J. Monroy, J.E. Siado, G.R. Snow, B. Stieger

State University of New York at Buffalo, Buffalo, USA

M. Alyari, J. Dolen, J. George, A. Godshalk, C. Harrington, I. Iashvili, J. Kaisen, A. Kharchilava, A. Kumar, A. Parker, S. Rappoccio, B. Roozbahani

Northeastern University, Boston, USA

G. Alverson, E. Barberis, D. Baumgartel, A. Hortiangtham, A. Massironi, D.M. Morse, D. Nash, T. Orimoto, R. Teixeira De Lima, D. Trocino, R.-J. Wang, D. Wood

Northwestern University, Evanston, USA

S. Bhattacharya, K.A. Hahn, A. Kubik, J.F. Low, N. Mucia, N. Odell, B. Pollack, M.H. Schmitt, K. Sung, M. Trovato, M. Velasco

University of Notre Dame, Notre Dame, USA

N. Dev, M. Hildreth, K. Hurtado Anampa, C. Jessop, D.J. Karmgard, N. Kellams, K. Lannon, N. Marinelli, F. Meng, C. Mueller, Y. Musienko³⁵, M. Planer, A. Reinsvold, R. Ruchti, G. Smith, S. Taroni, N. Valls, M. Wayne, M. Wolf, A. Woodard

The Ohio State University, Columbus, USA

J. Alimena, L. Antonelli, J. Brinson, B. Bylsma, L.S. Durkin, S. Flowers, B. Francis, A. Hart, C. Hill, R. Hughes, W. Ji, B. Liu, W. Luo, D. Puigh, B.L. Winer, H.W. Wulsin

Princeton University, Princeton, USA

S. Cooperstein, O. Driga, P. Elmer, J. Hardenbrook, P. Hebda, J. Luo, D. Marlow, T. Medvedeva, M. Mooney, J. Olsen, C. Palmer, P. Piroué, D. Stickland, C. Tully, A. Zuranski

University of Puerto Rico, Mayaguez, USA

S. Malik

Purdue University, West Lafayette, USA

A. Barker, V.E. Barnes, S. Folgueras, L. Gutay, M.K. Jha, M. Jones, A.W. Jung, K. Jung, D.H. Miller, N. Neumeister, B.C. Radburn-Smith, X. Shi, J. Sun, A. Svyatkovskiy, F. Wang, W. Xie, L. Xu

Purdue University Calumet, Hammond, USA

N. Parashar, J. Stupak

Rice University, Houston, USA

A. Adair, B. Akgun, Z. Chen, K.M. Ecklund, F.J.M. Geurts, M. Guilbaud, W. Li, B. Michlin, M. Northup, B.P. Padley, R. Redjimi, J. Roberts, J. Rorie, Z. Tu, J. Zabel

University of Rochester, Rochester, USA

B. Betchart, A. Bodek, P. de Barbaro, R. Demina, Y.t. Duh, T. Ferbel, M. Galanti, A. Garcia-Bellido, J. Han, O. Hindrichs, A. Khukhunaishvili, K.H. Lo, P. Tan, M. Verzetti

Rutgers, The State University of New Jersey, Piscataway, USA

J.P. Chou, E. Contreras-Campana, Y. Gershtein, T.A. Gómez Espinosa, E. Halkiadakis, M. Heindl, D. Hidas, E. Hughes, S. Kaplan, R. Kunnawalkam Elayavalli, S. Kyriacou, A. Lath, K. Nash, H. Saka, S. Salur, S. Schnetzer, D. Sheffield, S. Somalwar, R. Stone, S. Thomas, P. Thomassen, M. Walker

University of Tennessee, Knoxville, USA

M. Foerster, J. Heideman, G. Riley, K. Rose, S. Spanier, K. Thapa

Texas A&M University, College Station, USA

O. Bouhali⁶⁹, A. Celik, M. Dalchenko, M. De Mattia, A. Delgado, S. Dildick, R. Eusebi, J. Gilmore, T. Huang, E. Juska, T. Kamon⁷⁰, R. Mueller, Y. Pakhotin, R. Patel, A. Perloff, L. Perniè, D. Rathjens, A. Rose, A. Safonov, A. Tatarinov, K.A. Ulmer

Texas Tech University, Lubbock, USA

N. Akchurin, C. Cowden, J. Damgov, C. Dragoiu, P.R. Duerdo, J. Faulkner, S. Kunori, K. Lamichhane, S.W. Lee, T. Libeiro, S. Undleeb, I. Volobouev, Z. Wang

Vanderbilt University, Nashville, USA

A.G. Delannoy, S. Greene, A. Gurrola, R. Janjam, W. Johns, C. Maguire, A. Melo, H. Ni, P. Sheldon, S. Tuo, J. Velkovska, Q. Xu

University of Virginia, Charlottesville, USA

M.W. Arenton, P. Barria, B. Cox, J. Goodell, R. Hirosky, A. Ledovskoy, H. Li, C. Neu, T. Sinthuprasith, X. Sun, Y. Wang, E. Wolfe, F. Xia

Wayne State University, Detroit, USA

C. Clarke, R. Harr, P.E. Karchin, P. Lamichhane, J. Sturdy

University of Wisconsin - Madison, Madison, WI, USA

D.A. Belknap, S. Dasu, L. Dodd, S. Duric, B. Gomber, M. Grothe, M. Herndon, A. Hervé, P. Klabbers, A. Lanaro, A. Levine, K. Long, R. Loveless, I. Ojalvo, T. Perry, G.A. Pierro, G. Polese, T. Ruggles, A. Savin, A. Sharma, N. Smith, W.H. Smith, D. Taylor, N. Woods

†: Deceased

1: Also at Vienna University of Technology, Vienna, Austria

2: Also at State Key Laboratory of Nuclear Physics and Technology, Peking University, Beijing, China

3: Also at Institut Pluridisciplinaire Hubert Curien, Université de Strasbourg, Université de

-
- Haute Alsace Mulhouse, CNRS/IN2P3, Strasbourg, France
- 4: Also at Universidade Estadual de Campinas, Campinas, Brazil
 - 5: Also at Université Libre de Bruxelles, Bruxelles, Belgium
 - 6: Also at Deutsches Elektronen-Synchrotron, Hamburg, Germany
 - 7: Also at Joint Institute for Nuclear Research, Dubna, Russia
 - 8: Also at Cairo University, Cairo, Egypt
 - 9: Also at Fayoum University, El-Fayoum, Egypt
 - 10: Now at British University in Egypt, Cairo, Egypt
 - 11: Now at Ain Shams University, Cairo, Egypt
 - 12: Also at Université de Haute Alsace, Mulhouse, France
 - 13: Also at CERN, European Organization for Nuclear Research, Geneva, Switzerland
 - 14: Also at Skobeltsyn Institute of Nuclear Physics, Lomonosov Moscow State University, Moscow, Russia
 - 15: Also at Tbilisi State University, Tbilisi, Georgia
 - 16: Also at RWTH Aachen University, III. Physikalisches Institut A, Aachen, Germany
 - 17: Also at University of Hamburg, Hamburg, Germany
 - 18: Also at Brandenburg University of Technology, Cottbus, Germany
 - 19: Also at Institute of Nuclear Research ATOMKI, Debrecen, Hungary
 - 20: Also at MTA-ELTE Lendület CMS Particle and Nuclear Physics Group, Eötvös Loránd University, Budapest, Hungary
 - 21: Also at University of Debrecen, Debrecen, Hungary
 - 22: Also at Indian Institute of Science Education and Research, Bhopal, India
 - 23: Also at Institute of Physics, Bhubaneswar, India
 - 24: Also at University of Visva-Bharati, Santiniketan, India
 - 25: Also at University of Ruhuna, Matara, Sri Lanka
 - 26: Also at Isfahan University of Technology, Isfahan, Iran
 - 27: Also at University of Tehran, Department of Engineering Science, Tehran, Iran
 - 28: Also at Plasma Physics Research Center, Science and Research Branch, Islamic Azad University, Tehran, Iran
 - 29: Also at Università degli Studi di Siena, Siena, Italy
 - 30: Also at Purdue University, West Lafayette, USA
 - 31: Also at International Islamic University of Malaysia, Kuala Lumpur, Malaysia
 - 32: Also at Malaysian Nuclear Agency, MOSTI, Kajang, Malaysia
 - 33: Also at Consejo Nacional de Ciencia y Tecnología, Mexico city, Mexico
 - 34: Also at Warsaw University of Technology, Institute of Electronic Systems, Warsaw, Poland
 - 35: Also at Institute for Nuclear Research, Moscow, Russia
 - 36: Now at National Research Nuclear University 'Moscow Engineering Physics Institute' (MEPhI), Moscow, Russia
 - 37: Also at St. Petersburg State Polytechnical University, St. Petersburg, Russia
 - 38: Also at University of Florida, Gainesville, USA
 - 39: Also at P.N. Lebedev Physical Institute, Moscow, Russia
 - 40: Also at California Institute of Technology, Pasadena, USA
 - 41: Also at Faculty of Physics, University of Belgrade, Belgrade, Serbia
 - 42: Also at INFN Sezione di Roma; Università di Roma, Roma, Italy
 - 43: Also at Scuola Normale e Sezione dell'INFN, Pisa, Italy
 - 44: Also at National and Kapodistrian University of Athens, Athens, Greece
 - 45: Also at Riga Technical University, Riga, Latvia
 - 46: Also at Institute for Theoretical and Experimental Physics, Moscow, Russia
 - 47: Also at Albert Einstein Center for Fundamental Physics, Bern, Switzerland

- 48: Also at Adiyaman University, Adiyaman, Turkey
- 49: Also at Mersin University, Mersin, Turkey
- 50: Also at Cag University, Mersin, Turkey
- 51: Also at Piri Reis University, Istanbul, Turkey
- 52: Also at Gaziosmanpasa University, Tokat, Turkey
- 53: Also at Ozyegin University, Istanbul, Turkey
- 54: Also at Izmir Institute of Technology, Izmir, Turkey
- 55: Also at Marmara University, Istanbul, Turkey
- 56: Also at Kafkas University, Kars, Turkey
- 57: Also at Istanbul Bilgi University, Istanbul, Turkey
- 58: Also at Yildiz Technical University, Istanbul, Turkey
- 59: Also at Hacettepe University, Ankara, Turkey
- 60: Also at Rutherford Appleton Laboratory, Didcot, United Kingdom
- 61: Also at School of Physics and Astronomy, University of Southampton, Southampton, United Kingdom
- 62: Also at Instituto de Astrofísica de Canarias, La Laguna, Spain
- 63: Also at Utah Valley University, Orem, USA
- 64: Also at University of Belgrade, Faculty of Physics and Vinca Institute of Nuclear Sciences, Belgrade, Serbia
- 65: Also at Facoltà Ingegneria, Università di Roma, Roma, Italy
- 66: Also at Argonne National Laboratory, Argonne, USA
- 67: Also at Erzincan University, Erzincan, Turkey
- 68: Also at Mimar Sinan University, Istanbul, Istanbul, Turkey
- 69: Also at Texas A&M University at Qatar, Doha, Qatar
- 70: Also at Kyungpook National University, Daegu, Korea